Activation of Oxygen Nucleophiles in Enzyme Catalysis

Vernon E. Anderson,*,† Mark W. Ruszczycky,† and Michael E. Harris†,‡

Department of Biochemistry and the Center for RNA Molecular Biology, Case Western Reserve University, School of Medicine, Cleveland, Ohio 44106

Received January 17, 2006

Contents

1. Enhancing Alcohol Nucleophilicity

1.1. Introduction

Group transfer reactions, as shown in eq 1, represent a large class of enzyme catalyzed reactions.

$$RO{-}H + X{-}R_{LG} \rightleftarrows RO{-}X + H{-}R_{LG} \qquad (1)$$

In these reactions, the acceptor forms a new bond to the transferred group. When the bonding electrons are derived from the acceptor, it functions as a nucleophile in the reaction, while the atom of the transferred group is the electrophile, and the atom whose bond is cleaved constitutes the leaving group. Physical organic chemists have developed numerous tools that can be used to dissect the contributions of each of these three functionalities to the reactivity of the system. This review focuses on the application of these methods to enzyme reactions, to ascertain how the environment of the enzyme active site affects the reactivity of oxygen nucleophiles, with an emphasis on alcohols.

On the simplest level, there should be minimal variation in the nucleophilicity of different oxygen atoms; in every biologically relevant structure, every oxygen will have two accessible lone pairs of electrons, one of which would serve as the nucleophilic lone pair. This assertion, however, is demonstrably false, as the second-order rate constants for the reaction of oxygen nucleophiles can vary over 7 orders of magnitude in the standard displacement of halides from CH_3X.[1,2] Qualitatively, the fundamental mechanism of enhancing the nucleophilic power of any given oxygen atom is to enhance the electron density of the nucleophilic lone electron pair. This leads to three molecular mechanisms of generating enhanced electron density in the reactant state of the nucleophile by altering the coordination and/or bonding of the nucleophile: (1) desolvation, or more precisely the stripping of H-bond donors to the nucleophilic lone pair, (2) coordination of the alcohol proton, i.e., H-bonding to a general base, and (3) ionization, as shown in Figure 1. In addition to these three mechanisms, an electric field generated at the active site can polarize a bond to the nucleophile, enhancing its nucleophilicity. Moreover, enzymes reduce the order of the substitution reaction by simultaneously binding both the nucleophile and electrophile and can stabilize the nucleophilic transition state by general base catalysis. The potential importance of nucleophilic catalysis has been highlighted by Houk and co-workers.[3] In section 2, examples from several protein and RNA enzymes will be reviewed, and in section 3, methods of experimentally determining the electron density on nucleophilic alcohol oxygen atoms will be considered.

1.2. Effect of Variation of Electron Density on Alcohol Nucleophilicity

The electron density on alcohol oxygens can be varied molecularly by inductive or resonance effects. This variation in electron density is experimentally characterized by the pK_a of the neutral hydroxyl oxygen in aqueous solution; lower pK_a's correlate with lower electron density. The effects of the reduced electron density on the rate constants for nucleophilic reactions are often characterized by linear free energy correlations, plotting log k_{nuc} vs pK_a, as shown in Figure 2.

The slope of these lines is the Bronsted β, and if the base is functioning as a nucleophile, it is referred to as β_{nuc}. The interpretation of the data in Figure 2 is nontrivial, since the rate constants include contributions from both general base

* To whom correspondence should be addressed. E-mail: vea@case.edu. Phone: (216) 368-2599. Fax: (216) 368-3419.
† Department of Biochemistry.
‡ Center for RNA Molecular Biology.

10.1021/cr050281z CCC: $59.00
Published on Web 07/26/2006

Vernon E. Anderson received a B.S. in Chemical Engineering from the University of Missouri—Columbia and a Ph.D. in Biochemistry studying isotope effects with W. W. Cleland. Vernon's interests, in addition to determination of isotope effects by mass spectrometry, expanded to include the use of stable isotopes to characterize enzyme–substrate complexes by spectroscopic means. These interests were developed while he pretended to be an organic chemist for eight years at Brown University. With the development of electrospray and MALDI mass spectrometry, Vernon has found a wider scope for the application of stable isotopes as Professor of Biochemistry and Chemistry at Case Western Reserve University.

Mark W. Ruszczycky received his B.S. in Biochemistry and his M.S. in Chemistry from the University of California at Riverside. He then moved to Cleveland to earn his M.D. and Ph.D. degrees in the Medical Scientist Training Program at Case Western Reserve University. Currently, Mark is finishing his thesis work for the Ph.D. phase of his training by studying transition states in enzyme catalyzed nucleophilic displacements.

and nucleophilic catalysis as well as changes in the rate determining step from decomposition to formation of a tetrahedral intermediate. Nonetheless, the variation in rate constants of 6 to 8 orders of magnitude amply demonstrates the potential for catalysis achieved by altering the electron density on the nucleophilic oxygen atom.

Michael E. Harris attended Florida State University, where he received a B.S. degree in Chemistry in 1986, and he received a Ph.D. in Biochemistry from the University of Alabama in 1992 with Dr. Stephen Hajduk, working on RNA processing. Dr. Harris' interest in the chemistry of nucleic acids was further developed during postdoctoral work in the laboratory of Norm Pace at Indiana University. He is currently an Associate Professor at CWRU, where his laboratory focuses on mechanisms of RNA catalysis and the interactions of RNA with metal ions and protein. In addition to enzyme and RNA research, Dr. Harris spends his energy raising his teenage children and restoring their 100 year old home.

In biological nucleophilic reactions, the intrinsic nucleophilicity of the substrate cannot be altered, as the physiological role of the enzymatic transformation and the substrate specificity of most enzymes define the covalent structure of the alcohol nucleophile. It is possible that electric fields at an enzyme active site can alter the electron density and distribution on the nucleophilic oxygen to enhance its nucleophilicity. The size and direction of electric fields can be calculated,[5] and their effect on specific bonds within a substrate bound at an active site can be spectroscopically detected in favorable cases[6,7] (see also the Carey contribution to this thematic issue). An illustrative example is the variation in electron density on the nucleophilic O induced by phosphate binding to the active site of nucleoside phosphorylase observed by vibrational spectroscopy.[8] The vibrational spectra reveal that one of the three resonance equivalent P−O bonds of HPO_4^{2-}, presumably the bond to the nucleophilic O, becomes so polarized in the active site that its bond order is decreased from 1.31 to 1.23 with a concomitant increase in electron density of the nucleophilic O.

1.3. Desolvation

Oxygen nucleophiles are H-bond acceptors in protic solvents, and such interactions have a profound influence on their reactivity. Figure 1A emphasizes the potential deactivation of oxygen nucleophiles by H-bonding to aqueous solvent. A lone electron pair that is the acceptor of an H-bond

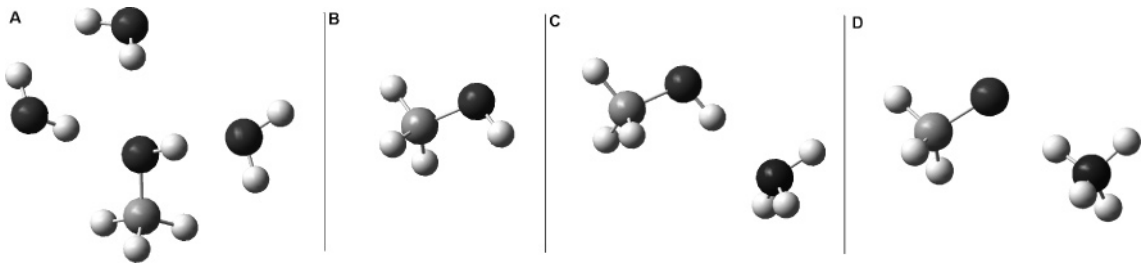

Figure 1. Three molecular mechanisms of activating methanol as a nucleophile are shown in the transitions: A → B shows transfer of H-bond donating solvent water molecules (A) to a desolvated molecule (B), B → C shows H-bond donation to form a complex with a general base, NH_3 in panel C, and C → D shows ionization where proton transfer results in methoxide and a protonated base.

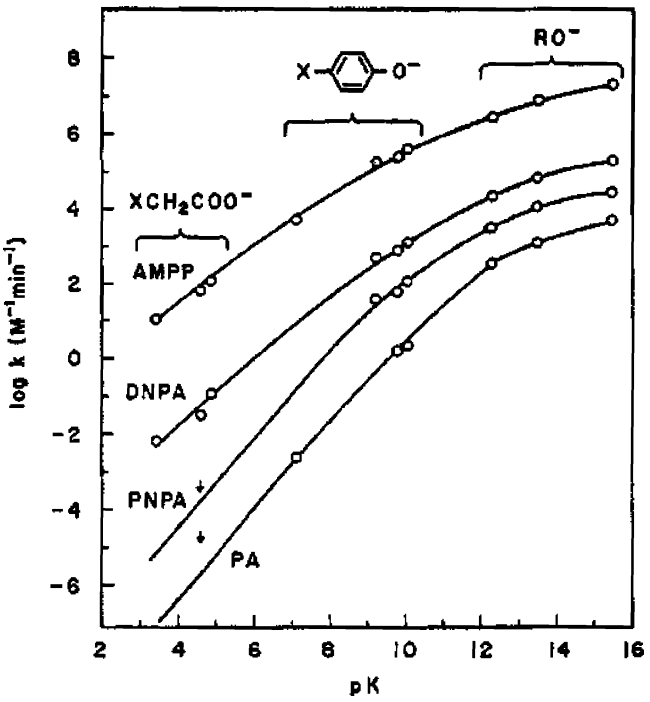

Figure 2. Second-order rate constants vs pK_a for the reaction of four different esters, phenyl acetate (PA), *p*-nitrophenylacetate (PNPA), dinitrophenyl acetate (DNPA), and 1-acetoxy-4-methoxypyridinium perchlorate (AMPP) vs the pK_a of three classes of ionized oxygen nucleophiles, substituted acetates (pK_a's 3−5), phenoxides (pK_a's 6−10), and halogenated alkoxides (pK_a's 12−16). Reproduced with permission from ref 4. Copyright 1968 American Chemical Society.

cannot be nucleophilic for both electronic and steric considerations. Consequently, prior to reaching the transition state for a nucleophilic displacement, the nucleophilic lone pair must lose any interaction with an H-bond donor. In addition to this primary requirement, H-bonding to a second lone pair (or third for oxyanions) can reduce the electron density on the nucleophilic lone pair.

To quantify the contribution of the specific solvation of oxygen nucleophiles by protic solvents, the rate constants for nucleophilic displacements in dipolar aprotic solvents have been compared to those in protic solvents. Increases between 10^4- and 10^7-fold, depending both on the nucleophile and on the electrophile, are routinely observed.[9] These very large rate enhancements are attributed to preferential solvation of the reactants relative to the transition states of the reactions. These effects will be greatest when the specific H-bond solvation of the nucleophile is greatest, i.e., alkoxides and other very basic anionic oxygen nucleophiles.

It has become possible to examine solvation effects by quantum chemical calculations.[10−13] To reproduce the effects of aqueous solvation, specific water molecules must be included in a supermolecule approach. Recent developments, generically termed QM/MM methods, have permitted the solvent molecules to be treated with molecular mechanics while the chemically reactive species are considered at the available quantum chemical level. A computational study that specifically analyzed the contribution of desolvation to the rate enhancement provided by DMSO relative to water concluded that removing the H-bond donating solvent molecules played a significant role in contributing to the rate enhancement.[11]

The second indication of the importance of desolvation in activating oxygen nucleophiles in aqueous solution comes from cases of a Bronsted linear free energy relationship (LFER) such as that shown in Figure 2. As the bases become stronger in Figure 2, the slope of the plot, i.e., β_{nuc}, decreases. As the anions of these bases are more strongly H-bonded to solvent, there is a greater energetic cost to desolvation prior to forming the transition state. This increased energetic demand offsets the increase in nucleophilicity projected for the stronger base and will consequently result in a decrease in β_{nuc}.[4,14] This effect has been demonstrated to apply to neutral nucleophiles as well as anionic nucleophiles.[15] This interpretation of curved Bronsted LFERs remains a prominent method to implicate a role for nucleophile desolvation in physical organic studies of reactions with biological relevance.[16,17]

Desolvation as a mechanism of nucleophile activation, however, remains contentious. As Warshel's group concludes from computational studies, it is not desolvation that enzymes use to effect catalysis but specific solvation of the transition state.[18,19] Warshel does not focus on the contribution of the solvent interaction with the nucleophile, as he adopts a more holistic approach, defining the solvation energy as the binding energy of the entire nucleophile and electrophile. This "solvation energy" is greater for transfer to the enzyme active site than for transfer to aqueous solution. This reactant state approach contrasts with the focus on the individual interactions with the nucleophilic oxygen atom. Experimentally or computationally, dissecting the specific energetic contribution from H-bonding to the nucleophilic water poses technical problems and will require greater care in definition than the too general term "desolvation". Nonetheless, the chemical imperative of removing the specific H-bond donors for nucleophilic reactions to occur, coupled with the crystallographic evidence that the nucleophilic lone pairs do not serve as H-bond acceptors in ternary enzyme structures, will continue to support the concept that this is one of the fundamental mechanisms employed by enzymes to promote catalysis.

1.4. H-Bonding to a General Base

General base catalysis, according to Jencks' libido rule, occurs "in complex reactions in aqueous solution only at sites that undergo a large change in pK_a in the course of the reaction, and when the pK_a of the catalyst is intermediate between the initial and final pK_a values of the substrate site."[20] This is shown in Figure 3 for an alcohol as the nucleophile. As the pK_a of the alcohol would decrease from $\sim$16 to $<$0 for a protonated ether, nucleophilic substitution by alcohols satisfies the libido rule if the pK_a of the general base lies anywhere between these two extremes. Somewhat surprisingly, there are few examples of complete Bronsted analyses of general base catalysis of alcohols as nucleophiles, in part because the alcohols compete poorly with water and/or hydroxide in aqueous solution. In those cases where the Bronsted β has been determined, the values range between 0.2 and 0.3.[21−23]

The Bronsted β value corresponds roughly to the fraction of proton transfer that has occurred in the transition state, i.e., the distance along the *x*-axis in the More O'Ferrall plot of Figure 3. Low values of Bronsted β are consistent with an early transition state and only partial transfer of the proton to the general base. However, all of the reactions characterized have very good leaving groups. In reactions with poorer leaving groups, later transition states and greater proton transfer to the general base would be anticipated. In

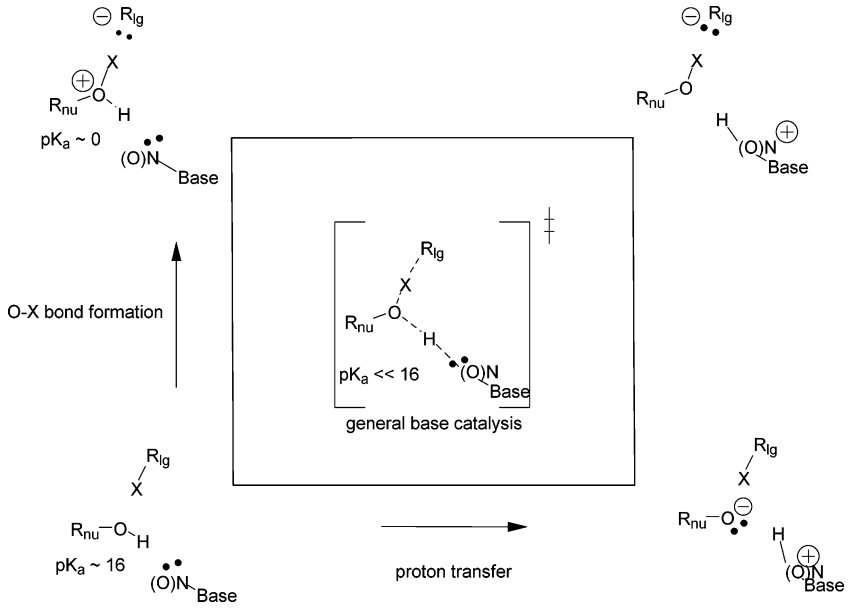

Figure 3. More O'Ferrall diagram comparing the extent of nucleophile−electrophile bond formation on the *y*-axis with proton transfer on the *x*-axis. General base catalysis, according to Jencks' libido rule, can occur when the pK_a of the base is between the pK_a of the nucleophile (∼16 for an alcohol) and that of the immediate product of the displacement reaction (the protonated ether, pK_a ∼ 0) shown on the *y*-axis. General base mechanisms have transition states in the interior of the More O'Ferrall diagram with the proton transfer concerted with formation of the nucleophilic O−X bond and cleavage of the O−R_{lg} bond. Specific base catalysis follows the perimeter along the bottom and right sides with the rate determining step corresponding to the nucleophilic displacement.

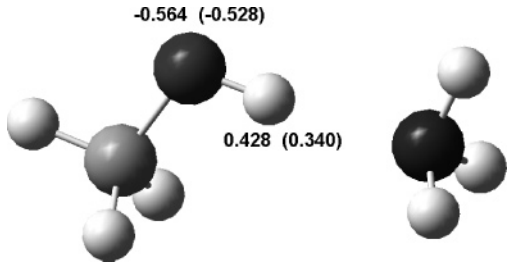

Figure 4. Mulliken charges on the methanol oxygen and hydrogen in the H-bond to ammonia determined at the B3LYP/6-31+G(d,p) level compared. The values for methanol alone in the gas phase are shown in parentheses, emphasizing the polarization of the O−H bond and the increase in electron density on the oxygen resulting from the formation of the H-bond.

computational studies of the ammonia and water promoted additions of methanol to formamide, effectively complete proton transfer from the alcohol to the general base was predicted.[24]

Independent of the position of the proton in the transition state, the donation of an H-bond by the alcohol O−H will enhance the electron density on the nucleophilic oxygen. This is most easily demonstrated computationally. In Figure 4, the presence of the electrons of the H-bond acceptor attracts the proton from the alcohol, decreasing the O−H σ-bond order. The result is an increased partial positive charge on the proton and an increase in negative charge on the nucleophilic oxygen, as suggested by the Mulliken charges calculated for methanol H-bonded to NH_3. This increase in electron density will increase the nucleophilicity of the oxygen and provides a mechanism of catalysis independent of whether there is complete proton transfer, i.e. general base catalysis, in the reaction. Experimental evidence for this effect can be found by NMR and vibrational spectroscopy (section 3).

The correlation of the geometry of the RO−H···acceptor H-bond in the reactant and transition states is an issue of significant interest. H-bond strength between an alcohol donor and a general base acceptor has been correlated with the distance between the heteroatoms in small molecule crystal structures[25] or by decreases in the O−H stretching frequency.[26] These spectroscopic/crystallographic parameters are technically problematic to obtain from enzyme−substrate complexes. The large background contributed by O−H bonds from solvent water and other functional groups in the protein makes spectroscopy difficult. Even high resolution crystal structures find it problematic to correctly place H-bonded protons of active site serine nucleophiles (cf. the 0.78 and 0.81 Å structures of serine proteases[27,28]). These problems combine to make general base promoted nucleophilicity perhaps the most highly cited but poorly characterized mechanism of enzyme catalysis. The problem of spectroscopically characterizing these H-bonds is the topic of section 3.

1.5. Ionization

Full deprotonation, or ionization, of an oxygen nucleophile in aqueous solution is identified as specific base catalysis and is readily recognized by determining a pH rate profile that breaks at the pK_a of the nucleophile. The presumption is held that carboxylates will always be bound in the ionized form when functioning as nucleophiles; for phenols, binding of the phenoxide is probable, and for alcohols, the neutral form will be bound and, subsequently, will require deprotonation. As shown in Figure 3, this deprotonation may occur after binding, as a result of specific base catalysis, or during the reaction, as general base catalysis.

Figure 3 emphasizes that the difference between general and specific base catalysis is in the timing of the proton transfer. This difference should be detectable by primary solvent deuterium kinetic isotope effects. A proton transfer prior to the nucleophilic substitution/addition step will be accompanied only by an equilibrium isotope effect that was initially estimated to be minimal for proton transfers from

O−H to O or N acceptors.[29] However, if the proton transfer occurs by general base catalysis during the nucleophilic step, there would be a comparatively large primary deuterium kinetic isotope effect. Primary deuterium kinetic isotope effects are routinely in the range of 4−6 and in the presence of tunneling can be significantly larger. A large number of D_2O kinetic isotope effects have been determined for enzymes catalyzing nucleophilic reactions of alcohols, and surprisingly, the observed effects are rarely larger than 2−3. To account for the small solvent kinetic isotope effects observed, Schowen and Limbach, elaborating on proposals of Swain et al.[21] as well as Kreevoy and Cordes,[30,31] have proposed that, while proton transfer occurs during the nucleophilic reaction, the proton remains in a normal potential well and proton transfer is not coupled to the reaction coordinate.[32] Additional complications that contribute to the difficulty in interpreting solvent kinetic isotope effects derive from the large equilibrium isotope effects of ~2.5 that accompany the formation of strong low barrier H-bonds.[33] Thus, the modest D_2O kinetic isotope effects that are routinely observed are consistent with the formation of a strong low barrier H-bond in the transition state rather than actual proton transfer.

In hydrolysis reactions, where water is the nucleophile, coordination to metal ions which promotes ionization and localizes the nucleophilic oxygen is common. To promote ionization of alcohols, however, there are few examples of metal ion coordination; the examples of pyruvate kinase coordinating the enolate of pyruvate[34,35] and catechol *O*-methyltransferase (COMT) where the ionized catechol substrate is stabilized by the Mg^{2+} present at the active site (see section 2.5) are notable exceptions.[36]

In summary, physical organic chemistry provides clear evidence that small increases in electron density on nucleophilic oxygen atoms can result in dramatic rate enhancements for nucleophilic displacements. The process of increasing the electron density of an oxygen nucleophile, particularly of an alcohol, can be viewed as the sequential removal of protons. The initial step is removing solvent waters that donate H-bonds, thus generating the requisite "desolvated" nucleophilic lone pair of electrons. The second step is to coordinate the O−H proton, and the final step is complete transfer of the proton to an acceptor. Crystal structures of enzymes have provided strong evidence for the first two steps, but kinetic, spectroscopic, and computational methods will be required to quantify the strength of the interactions and to determine their timing relative to nucleophilic bond formation.

2. Nucleophilic Activation of Alcohols by Enzymes

Nucleophilic displacements, as shown in eq 1, constitute an important class of reactions in biological systems and are catalyzed by protein and RNA enzymes. They play an integral role in signal transduction pathways mediated by protein kinases; they are prevalent in nearly all metabolic pathways and are necessary for the timely degradation and turnover of cellular components. Primary alcohols represent one type of nucleophile in these reactions and are exemplified by the hydroxymethylenes of sugars and the amino acid serine. Structural characterization has demonstrated that the bound nucleophiles have been stripped of solvent water while biochemical investigations of the enzymatic properties responsible for the activation of primary alcohols have focused primarily on pH and mutational analyses along with solvent isotope effects, establishing the requirement for a proton acceptor in most of these reactions. Studies of cyclic-AMP-dependent protein kinase (PKA), serine *O*-acetyltransferase (SAT), hexokinase, the serine proteases, and catechol *O*-methyltransferase (COMT) are presented in approximate order of increasing apparent activation of the nucleophilic oxygen. Additionally, RNA enzymes or ribozymes in biology also catalyze nucleophilic displacement involving nucleophilic activation of ribose hydroxyl groups, and the mechanisms of two exemplary systems, the GI self-splicing intron and the HDV ribozyme, are discussed and contrasted with protein catalysis.

2.1. Cyclic-AMP-Dependent Protein Kinase

Protein kinases are a pervasive group of enzymes that catalyze reactions particularly important in various signal transduction pathways. The prototypical reaction catalyzed by the protein kinases is transfer of the γ-phosphate of ATP to the hydroxyl group of a serine, threonine, or tyrosine residue in a target substrate protein. Thus, the enzymes may function, at least in part, to increase the nucleophilicity of the hydroxyl group in order to effect catalysis. Due to its role in a large number of biologically important processes, one of the most thoroughly studied enzymes in this group is PKA, which has received an extensive review by Adams.[37]

PKA catalyzes the transfer of the γ-phosphate of ATP to a serine or threonine hydroxyl in the consensus sequence Arg-Arg-X-Ser/Thr-Y, where X is a small residue and Y is a hydrophobic residue.[37−39] Catalysis is in part attributable to the removal of solvent H-bonds from the nucleophilic O of the serine as well as its H-bonding to the conserved active site aspartate, Asp166,[37,40−42] as shown in Figure 5.

While the Asp166 residue is known to enhance the catalytic rate of PKA, it is not essential, since mutation of the aspartate residue to alanine reduces the k_{cat} value approximately 300-fold.[45] Similar rate reductions have also been seen with aspartate mutations to alanine and asparagine in phosphorylase kinase.[46] Changes in the K_M values for the peptide substrates were either unaffected or increased by no more than 4-fold with these mutations.[45,46] Based on these results, the role of the Asp166 is primarily to enhance the catalytic power of the kinase with only a minor contribution to substrate binding.[37,45,46] This role as a putative general base has thus been evaluated along a continuum of possible transition state structures where at one end it is responsible for nearly complete ionization of the nucleophilic hydroxyl in the transition state, while at the other end it aids in orienting the hydroxyl for attack, accepting the proton late along the reaction coordinate.[37,47]

Determination of the pH dependence of the steady-state parameters for PKA demonstrated reduction in $V/K_{peptide}$ at low and high pH, indicating the presence of residues necessary to catalysis with pK_a values of 6.5 and 8.5.[48] This further implicated Asp166 as a general base involved in abstracting the hydroxyl proton during in-line attack on the γ-phosphate.[48−50] However, subsequent studies have indicated that it is not the active site aspartate which is being titrated but rather other ionizable groups necessary for substrate recognition.[51] While this decreased the importance of the active site aspartate as a general base necessary for ionizing the nucleophilic hydroxyl in the transition state, it does not rule it out, since the steady-state kinetics of PKA are limited by the ADP dissociation step rather than phosphoryl transfer.[52,53]

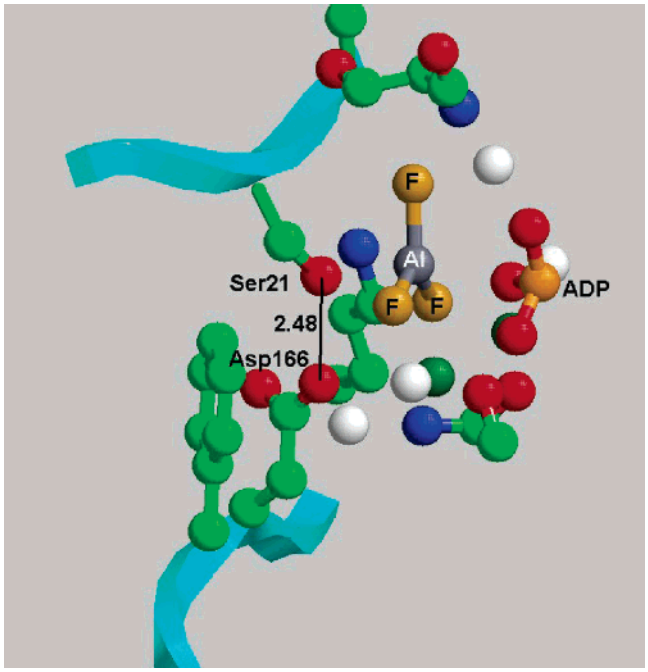

Figure 5. Crystal structure of cAMP-dependent protein kinase with a substrate peptide, and ADP with AlF_3 bound as a transition state analogue, adapted from protein database structure 1L3R[43] using RasTop.[44] The atoms of the substrates and key active site residues are shown as balls-and-sticks, carbon is light green, Mg^{2+} is dark green, and crystallographic waters are white spheres. The protein backbone is represented as a ribbon cartoon colored cyan. The activation of the nucleophilic serine is shown where the only H-bond donor/acceptor closer than 4.0 Å is Asp166, which is inferred to accept an H-bond from the nucleophilic Ser. The Cβ−O−Al angle is 109°, consistent with an in-line displacement by an oxygen lone pair.

Attempts to circumvent this problem have focused on the pre-steady-state kinetics of PKA.[47,53] Grant and Adams observed an initial burst of activity attributable to the initial phosphoryl transfer with an intrinsic rate constant of 500 s^{-1} followed by a slow linear reaction rate-limited by product release.[53] It was then discovered by Zhou and Adams that the burst phase was independent of both pH and solvent isotopic composition even when the phosphoryl transfer step was slowed by replacing Mg^{2+} with Mn^{2+}.[47] The lack of a solvent deuterium isotope effect suggests that the transferred proton resides in a stable bonding interaction with either the nucleophilic hydroxyl or some other atom in the transition state complex.[21,47,54] The pH independence indicated either a lack of general base catalysis or a base with a pK_a below 5.[47] Such a residue would be unable to deprotonate the nucleophilic hydroxymethylene prior to considerable O_{serine}−$P_{\gamma-phos}$ bond formation.[47] The independence of burst kinetics on solvent D_2O and pH is thus indicative of proton transfer likely taking place late in the formation of the O_{serine}−$P_{\gamma-phos}$ bond.[47]

The role of Asp166 has been investigated computationally. In the absence of Asp166, DFT computations identified a transition state stabilized by substrate assisted catalysis. The identified transition state was consistent with prior proton transfer, as the O_{serine}−H bond distance of 1.40 Å was significantly longer than the $O_{\gamma-phos}$−H distance of 1.07 Å,[55] which corroborated earlier semiempirical calculations.[56,57] Inclusion of Asp166 in postminimization refinement demonstrated a reduction in activation energy compared to the case of its absence.[55] These two results suggest that proton transfer from the serine hydroxyl is an important facet of the catalytic mechanism.

Two more recent *ab initio* calculations of the transition state for phosphoryl transfer in the active site at the DFT level of theory that included Asp166 both showed a dissociative transition state with Ser O−H bond lengths of 1.0 Å and H-bond distances of 2.5−2.6 Å to Asp166 and product structures where Asp166 was protonated.[58,59] Based on these results, both groups concluded that the active site aspartate is necessary for helping substrate bind, accepting the proton late during nucleophilic attack, and acting as a mediator in the transfer of the proton from the hydroxyl group to the phosphate following nucleophilic attack.[58,59] A third computational study using DFT QM/MM methods to model the entire enzyme complex rather than cluster models limited to just the active site residues further supports the role of the catalytic aspartate as a late proton acceptor.[60] It was also shown in this calculation that removal of the aspartate had no effect on the orientation of the nucleophilic hydroxyl group, indicating it functioned primarily as a proton trap.[60]

Current results for the reaction catalyzed by PKA support the hypothesis that the transition state for nucleophilic attack by serine involves minimal O_{serine}−H bond cleavage. The primary source of nucleophile activation remains removing any solvent water H-bonds. The very late proton transfer would correspond to a small β_{nuc}, indicating that increasing the proton affinity of Asp166 would not contribute significantly to the enzyme activity. Nevertheless, the active site aspartate contributes to nucleophilic activation as a general base primarily to accept the proton that is being released late along the reaction coordinate and to act as an intermediary in the protonation of the phosphoserine product.

2.2. Serine O-Acetyltransferase

SAT is a mechanistically well studied member of the left-handed β-helix family of acyltransferases which catalyze the transfer of the acetyl moiety of acetyl-CoA to a nucleophilic alcohol.[61] SAT catalyzes the transfer to the hydroxymethylene of L-serine to form *O*-acetyl-L-serine as part of the bacterial cysteine biosynthetic pathway.[62,63] As in the case of the protein kinases, studies on the catalytic properties of SAT suggest that nucleophilic activation involves a general base; however, the detailed role of the general base is still poorly understood.

The most direct evidence for the presence of a catalytic base comes from a combination of crystallographic and pH studies. Structural studies on the enzymes from *Haemophilus influenzae* and *Escherichia coli* complexed with the competitive inhibitor cysteine place two histidyl residues, His154A and His189B in *H. influenzae*, within H-bonding distance of the cysteine thiol.[64,65] As shown in Figure 6, His154A not only forms an H-bond to the thiol via its Nϵ2 but also is part of a catalytic dyad formed by an H-bond between its Nδ1 and the active site aspartate, Asp139B,[64,65] similar to that seen in the serine proteases (see below).[66,67] His154A has thus been proposed to serve as an active site general base to activate serine as a nucleophile for attack at the carbonyl carbon of acetyl-CoA.

His189B is believed to stabilize the resulting tetrahedral intermediate. Its H-bonding to the thiol of cysteine is likely a result of the larger S−H bond distance compared to that of O−H. It is this extra H-bonding that is believed to be responsible for the lower dissociation constant of cysteine versus serine and the lack of nucleophilic activation of the

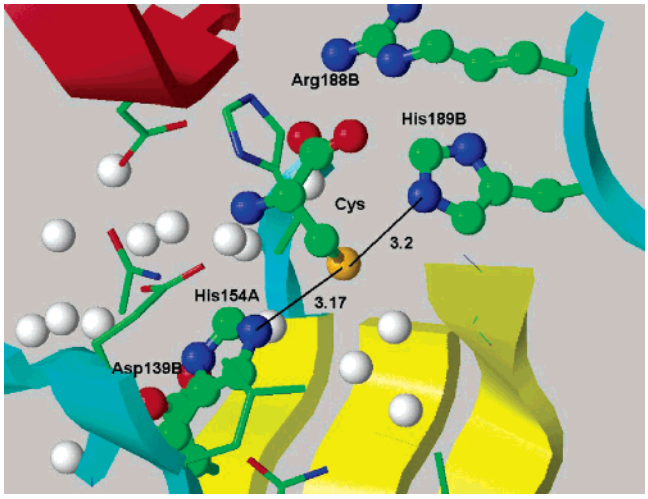

Figure 6. Heavily hydrated active site of SAT adapted from 1SSQ[62] using RasTop[44] with the atom representation defined in Figure 5 and the protein backbone appearing as a ribbon colored cyan for coil, red for helix, and yellow for β-strands. The H-bond distances between the substrate cysteine (Cys) and the two active site His residues are shown. Even in the absence of the second substrate, acetyl-CoA, the only H-bonds to the nucleophile are from the two His residues, as all of the water molecules are in excess of 4.0 Å from the sulfur.

cysteine thiol as an acetyl acceptor, explaining why cysteine is an effective competitive inhibitor, and not an alternative substrate, of the enzyme.[64,65,68,69] Evidence for two different H-bonding geometries has been obtained from Raman crystallography of [2$-^2$H$_2$]Cys bound at the active site, as there are at least four C$-$D stretching frequencies observed, all red-shifted from the frequencies observed in solution (Maiti, Roderick, Carey, and Anderson, unpublished).

Evaluation of the pH dependence of the steady-state parameters of SAT from *H. influenzae* also is indicative of general base catalysis. The enzyme demonstrates reduced activity at low pH but not in alkaline solution with acidic pK_a values of approximately 7 for V, V/K_{serine}, and $V/K_{acetyl\text{-}CoA}$.[70] Furthermore, other acyltransferases such as UDP-*N*-acetylglucosamine acyltransferase[71] and chloramphenicol acetyltransferase[72] show a reduction of catalytic activity upon mutation of the homologous histidines to alanines. However, mutation of the histidine in chloramphenicol acetyltransferase to glutamate produced an enzyme that retained some activity as measured by k_{cat} and almost no change in the K_M values for either chloramphenicol or acetyl-CoA, suggesting a catalytic requirement for an active site base.[72,73] These observations indicate that the active site His154A residue of SAT is necessary for full enzymatic activity and implicates it as a general base.[61]

Despite the apparent necessity of the unprotonated His154A residue for catalytic activity in SAT, its role in the activation of the nucleophilic γ-hydroxyl of serine is still uncertain. For the *H. influenzae* enzyme, proton inventory experiments indicate a single proton transfer during nucleophilic attack; however, the ^{D_2O}V and $^{D_2O}(V/K_{serine})$ solvent isotope effects were measured as 1.9 $\pm$ 0.2 and 2.5 $\pm$ 0.4, respectively.[70] The authors suggest that the V/K isotope effect reflects the intrinsic isotope effect for proton transfer from the serine hydroxyl to His154A, whereas the V isotope effect is diminished due to a commitment caused by slow dissociation of CoA, the second product released.[70] This being the case, the intrinsic isotope effect of 2.5 is small when compared to kinetic isotope effects in the range 6$-$10 that reflect proton transfers that are unbonded in the transition state.[21,54] Thus, the measured $^{D_2O}(V/K_{serine})$ suggests that proton transfer is asynchronous with tetrahedral intermediate formation. As noted in section 1.5, modest solvent isotope effects such as that observed here can arise from the transferring proton remaining in a stable vibrational well.

Secondary deuterium isotope effects on V/K_{serine} have also been measured for both the *pro-R* and *pro-S* β-hydrogens in the serine nucleophile using isotope ratio mass spectrometry.[74,75] Both effects, found to be nearly unity, are interpreted as being reflective of the nucleophilic transition state based on the absence of commitments determined in the solvent isotope effect study.[70] Since these effects are not significantly normal, any decrease in the serine O$-$H bond order must be compensated for by an increase in the incipient O$-$C bond order. His154A appears to act as a general base during nucleophilic attack; however, the modest solvent isotope effect suggests that the proton is transferred in a stable vibrational potential with a fractionation factor of $\sim$2.5 (see section 1.5) and that the nucleophilic serine hydroxyl is not ionized prior to attack at the carbonyl carbon.

2.3. Hexokinase

Hexokinase catalyzes the transfer of the γ-phosphate of ATP to the C6-hydroxyl of glucose, initiating the glycolytic pathway. Due to its central role in metabolism, it has also received considerable attention with regard to its catalytic mechanism. Like PKA and other kinases, it possesses an active site aspartyl residue, Asp189 in yeast hexokinase B, within H-bonding distance of the nucleophilic hydroxyl of glucose that is likewise believed to function as a general base.[76]

The steady-state parameters of hexokinase exhibit the decreases in V and V/K at acidic pH expected for general base catalysis.[77,78] Additionally, the measured acidic pK_a of 6.15 was found to increase upon addition of the organic solvent DMF to cationic-acid buffered solution, helping to assign the active site aspartate to the catalytic role.[77] Mutation of the active site aspartyl residue to alanine in human hexokinase likewise leads to reductions in V and V/K to less than 1% of the corresponding parameters of the wild-type enzyme.[79] The corresponding mutation in rat liver glucokinase yielded an enzyme with a 500-fold reduction in k_{cat}, but with little change in the K_M values for either glucose or ATP.[80] These results help to confirm the catalytic role of the active site aspartyl residue as a general base.

As in the case of PKA, measurements of solvent deuterium isotope effects on hexokinase are complicated by the phosphoryl transfer step not being as rate determining as those corresponding to product dissociation and conformation rearrangement,[81] which also exhibit solvent deuterium isotope effects.[82,83] Some headway has been made, however, by the measurement of secondary tritium equilibrium binding isotope effects at C6 of the glucose substrate using the method of ultrafiltration and human brain hexokinase.[84$-$86] These measurements have demonstrated a normal equilibrium isotope effect of 6.5% for the binding of [6,6-^{3}H$_2$]glucose to the enzyme alone[85] and 3.4% for forming the ternary complex in the presence of β,γ-CH$_2$-ATP, which correspond to deuterium effects of 4.6% and 2.4%, respectively.[86] The reduction in the isotope effect in the presence of the ATP analogue was proposed to result from coordination of the hydroxyl lone pair electrons with the phosphorus center of the γ-phosphate in the ternary Michaelis complex.[86] These

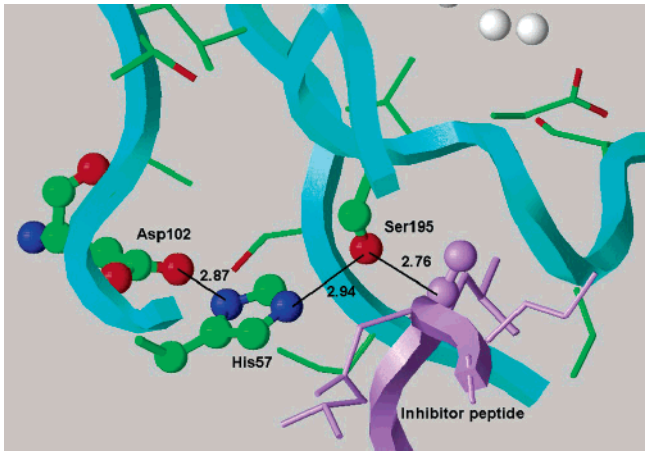

Figure 7. Catalytic triad of α-chymotrypsin adapted from the protein database coordinates for 1ACB[94] using RasTop[44] with defaults defined in Figure 5. Ser195 donates an H-bond to His57 and approaches a carbonyl carbon (purple sphere) of the inhibitor peptide (purple).

binding effects are of the same magnitude as the measured deuterium equilibrium isotope effect between the α- and *β*-anomers of glucose at the C1 position of 4.6%.[87] The molecular origin of these effects is discussed in section 3.3.

These binding isotope effects are still small when compared to calculated effects on ionization and/or strong H-bond formation. Calculations on isopropanol in the gas phase suggest normal *β*-secondary tritium isotope effects up to 60% for complete ionization and 20% for H-bonding with formate, depending on how the HC6−OH torsion angle changes upon H-bond formation.[84,87,88] Furthermore, these equilibrium effects do not indicate the nature of the interaction between the active site base and the nucleophilic hydroxyl group in the transition state. Therefore, while there does appear to be an H-bond between the active site aspartate of hexokinase and the C6 hydroxyl group, the nucleophilic hydroxyl is not significantly ionized in the Michaelis complex and the role of this interaction in the transition state remains to be clarified.

2.4. Serine Proteases

The serine proteases constitute a broad class of enzymes that cleave peptide bonds by way of an acyl-enzyme intermediate, and a comprehensive review of these enzymes has been written by Hedstrom.[67] The nucleophile in these reactions is an active site serine which attacks at the carbonyl carbon of the peptide bond to be cleaved, generating a tetrahedral intermediate which subsequently collapses to form an acyl-enzyme, thereby expelling the C-terminal fragment of the original peptide.[66,67,89,90] The acyl-enzyme is then hydrolyzed, expelling the N-terminal fragment of the peptide and regenerating the active deacylated form of the protease.[66,67,89,90] One of the most extensively studied members of this class of enzymes is α-chymotrypsin, which is discussed below as a representative example.

The active site nucleophile of α-chymotrypsin responsible for initial attack at the peptide bond is Ser195,[66] shown in Figure 7. In the presence of an inhibitor peptide, the serine participates in a single H-bond to His57, with a desolvated lone electron pair directed at an angle of ∼109° toward the carbonyl carbon of the inhibitor. The rate constant for enzyme acylation decreases below a pK_a of approximately 7, which was attributed to His57 following its identification in the first crystal structure of a serine protease. A requirement for a deprotonated His that is H-bonded to the nucleophile in the crystal structure suggested general base catalysis.[91−93] Further support for assigning this pK_a to His57 came from the observation of a solvent deuterium equilibrium isotope effect on this pK_a.[91] In addition to the interaction with the nucleophilic serine hydroxyl, His57 interacted via an H-bond to Asp102, forming the much studied "catalytic triad".[66]

The precise mechanism of how the catalytic triad activates Ser195 is the subject of a still unresolved debate. However, nearly all investigations to this end have focused primarily on the role of proton motion between His57 and Asp102 during catalysis rather than the transition state structure of Ser195 during the initial attack. Nevertheless, attempts to discriminate between one proton and two proton transfer mechanisms have provided some insight into how the serine is being activated.

Unlike the cases of SAT and hexokinase, isotopic labeling of the Ser195 residue of α-chymotrypsin and subsequently measuring secondary deuterium kinetic isotope effects is a technically daunting task. For this reason, most work has focused on solvent deuterium isotope effects. The first set of such experiments used the non-natural ester substrates *p*-nitrophenyl acetate and *p*-nitrophenyl trimethylacetate to determine the rate constants for serine acylation in both H_2O and D_2O using steady-state and pre-steady-state techniques.[91,95] The results indicated an intrinsic solvent deuterium isotope effect on acylation of 2.2[91,95] and a $^{D_2O}(k_{acylation}/K_M)$ isotope effect of 1.68.[95] These results indicated that general base catalysis was likely to be operant as opposed to unassisted nucleophile catalysis[95,96] and that there was a significant inverse isotope effect on K_M, interpreted as an equilibrium binding isotope effect of approximately 0.76 due to solvent−solvent interactions.[95] While the magnitudes of these effects are comparable to those of other nonenzymatic general base-catalyzed nucleophilic attacks, they once again are small compared to those of reactions involving nonenzymatic direct proton abstraction.[54,96]

It is also of interest that solvent deuterium isotope effects of similar magnitude were also found for other aspects of the α-chymotrypsin reaction. The intrinsic solvent isotope effect for deacylation of *trans*-cinnamoyl-α-chymotrypsin was measured as 2.5 while that for trimethylacetyl-α-chymotrypsin was 3.0.[95] Likewise, ^{D_2O}V for the ester substrate *N*-acetyl-L-tryptophan methyl ester was 2.8 for deacylation.[95] These values again suggest that, compared to the case of purely nucleophilic reactions, proton abstraction influences the reaction coordinate but that either proton abstraction from serine is asynchronous with the transition state for acylation or it is being transferred in a stable vibrational well (see section 1.5).

Later work on the serine proteases focused primarily on investigating the role of the catalytic triad. These studies utilized proton inventory measurements as a means to discriminate between one and two proton transfer mechanisms and in the process determined the solvent deuterium isotope effects for these transfers. One of the main discoveries of this work was that with substrates that made minimal contacts with the active site, e.g. nitrophenylacetate, a single proton transfer was found, while with more natural amide substrates simultaneous two proton transfer catalysis was suggested.[97] Measurements of the acylation reaction with the substrate *N*-acetyl-L-tryptophanamide demonstrated a proton

inventory consistent with two proton transfer and a ^{D_2O}V effect of ~2.0 with intrinsic effects of 1.69 and 1.14 for each of the two transfers.[91,97]

Interpretation of these effects is difficult due to the complexity of the reaction catalyzed by α-chymotrypsin. Although acylation is generally believed to be rate limiting for the hydrolysis of amides,[98] this assumption has been questioned.[67] Furthermore, acylation itself exhibits two transition states: nucleophilic attack forming a tetrahedral intermediate followed by collapse to form the acyl-enzyme. Transient kinetic and pH variation experiments on elastase and α-lytic protease have implied that the latter may be the rate-limiting step[99] or that His57 may be acylated prior to an N → O acyl shift to Ser195.[100] While many mechanistic possibilities exist, isotope effects of similar magnitude have been found for other serine proteases.[101−103] Thus, the general conclusion has been that mobilization of the catalytic triad for either single or double proton transfer depends on both the enzyme and the substrate but that the primary deuterium isotope effect on proton transfer from Ser195 to His57 during nucleophilic attack is small compared to values observed for direct nonenzymatic proton transfers.

Recently, QM/MM calculations by Ishida and Kato have analyzed the acylation reaction using the serine protease trypsin as the model system.[104] Their results using a peptide substrate indicate that a single proton transfer mechanism is favored with the Asp102 functioning to stabilize the His57 cation, rather than to deprotonate it, and orient it for interaction with Ser195. They also found that proton transfer between Ser195 and His57 is nearly complete in the transition state. This result is in contrast to the results for the enzymes described above, where the *ab initio* calculations suggested that deprotonation trailed formation of the covalent bond between the nucleophile and electrophile. Nevertheless, the early deprotonation is still consistent with the small solvent deuterium isotope effects. It is notable, however, that when the Asp102 is mutated to asparagine, the molecular dynamics QM/MM calculations resulted in minimal deprotonation in the acylation transition state of trypsin and, consequently, the proton transfer followed nucleophile bond formation in this mutant.[105]

2.5. Catechol O-Methyltransferase

COMT catalyzes the transfer of a methyl group from the activated electrophile, *S*-adenosyl methionine, to a phenolic oxygen. Phenolic oxygens are intrinsically less reactive than alcohol or water oxygens (when both are neutral) due to the delocalization of the lone pair electrons into the aromatic ring.[106,107] Therefore, it is anticipated that the ionized phenolate may be the actual substrate form in COMT. The resonance of the phenoxide electrons into the aromatic ring lowers the pK_a of phenolic oxygens to ~10. This resonance delocalization results in the *ortho* and *para* carbons becoming nucleophilic.[106,108] An enzyme active site, consequently, may need both to promote the ionization of the phenol and to minimize the potential for reaction at the *ortho* carbon. In COMT, these two tasks are accomplished by coordination of the phenol to an active site Mg^{2+} ion as shown in Figure 8.

COMT has been the focus of numerous experimental and computational studies to determine whether nucleophilic substitution reactions are promoted at enzyme active sites by compression[110,111] or proximity.[112] Initial studies indicated that general base catalysis in aqueous solution could promote

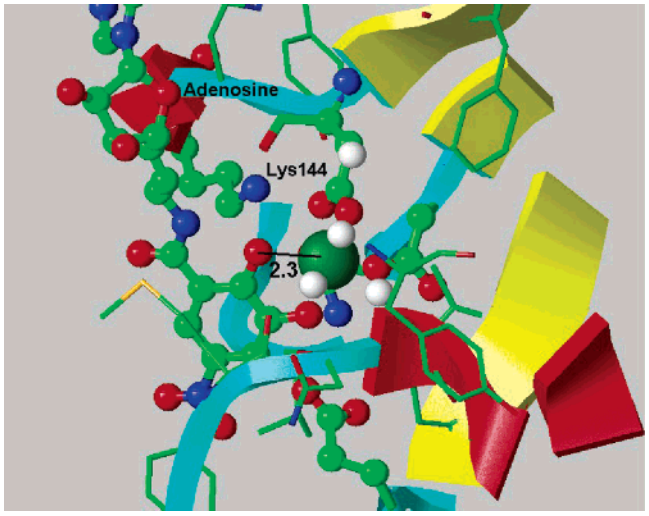

Figure 8. Active site of COMT derived from 1JR4[109] using RasTop[44] with defaults defined in Figure 5. The nucleophilic O of the inhibitor is identified by its proximity to the adenosine binding site, where the furanose O is labeled. The 2.3 Å distance between this O and the Mg^{2+} is indicated.

the reaction of phenols and catechols with sulfonium ions,[113] but coordination of the substrate to the active site Mg^{2+} coupled with the pH variation of $V/K_{catechol}$ have focused attention on the ionized catechol as the reactive form of the substrate bound at the active site. Still, as shown in Figure 9, three different reactive conformations of the catechol have been obtained computationally by the Kollman,[114] Bruice,[115] and Williams[116] groups. These three different structures highlight the need for experimental approaches to determine the environment of the nucleophilic O both in the Michaelis complex and in the transition state for the chemical reaction.

Metal ion coordination in the activation of water as a nucleophile is widely observed, and entire superfamilies of metal ion promoted hydrolysis reactions are being studied.[117] However in the promotion of the nucleophilicity of alcohols COMT and pyruvate kinase[35] are notable for the coordination of the nucleophilic O by a metal ion. Two additional classes of enzymes that invoke metal ion coordination of an alcohol O as the nucleophile are the nucleic acid polymerases and enzymes that catalyze phospho-transesterification, which will be discussed in the following sections.

2.6. Ribozyme Catalysis

The discovery by Cech and colleagues that RNA too can act as an enzyme was a key advance in our understanding of biological catalysis. We now know that most ribozymes found in biology catalyze substitutions at phosphorus that necessitate activation of an oxygen nucleophile. The same chemical principles that describe nonenzymatic and protein catalyzed reactions must necessarily hold true for RNA enzymes as well. The phospho-transesterifications catalyzed by ribozymes are effectively symmetrical, as shown in Figure 10. Specific acid, specific base, metal ion coordination, and general base mechanisms are diagrammed.

Due to the ability of RNA to fold into a variety of complex structures, RNA tertiary structure can generate crevices necessary for water exclusion, orient the substrates, coordinate metal ions, and provide specific noncovalent interactions with the transition state.[118−120] As a polyanion, RNA is particularly adept at divalent metal ion interactions.[121] RNA shares with protein enzymes that catalyze phosphoryl transfer

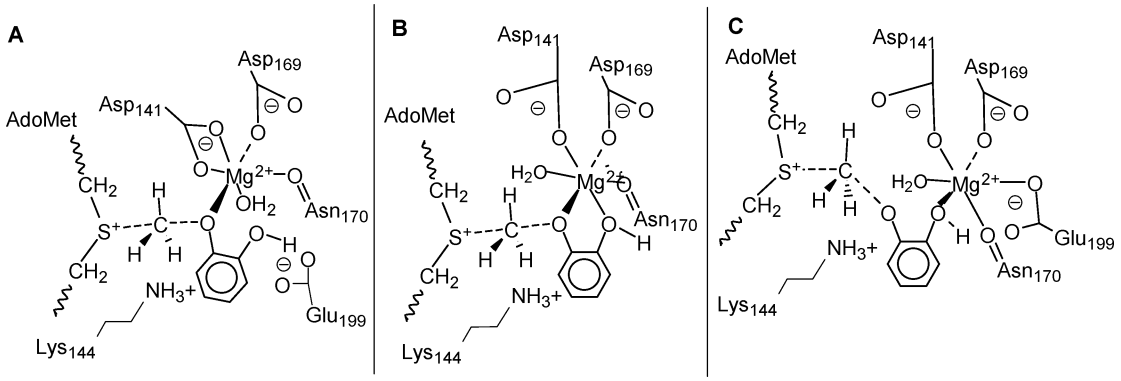

Figure 9. Three computational results of nucleophile activation by coordination to the active site Mg^{2+}: (A) The Kollman group's transition state structure with only the nucleophilic O of the catechol coordinated to the Mg^{2+}.[114] (B) The Bruice group's structure with both O atoms coordinated to the Mg^{2+}.[115] (C) The Williams group's structure with the nucleophilic O ionized but only the non-nucleophilic O coordinated to the Mg^{2+}.[110]

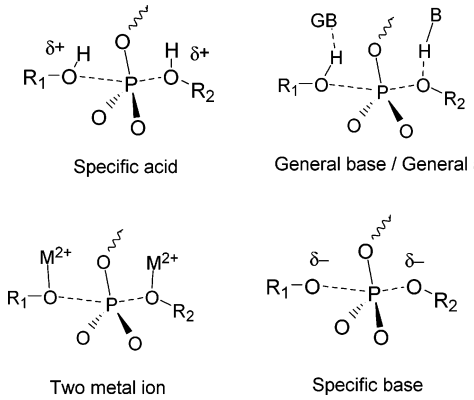

Figure 10. Four symmetrical transition states for phosphotransesterification that correspond to the different mechanisms for promoting nucleophilicity of the ribose OH, R_1-OH. Specific acid catalysis of the leaving group requires only desolvation of the nucleophile, general acid/base catalysis results in greater nucleophile activation, metal coordination in the two-metal ion mechanism results in pre-equilibrium deprotonation of the nucleophile, and specific base catalysis generates an alkoxide nucleophile.

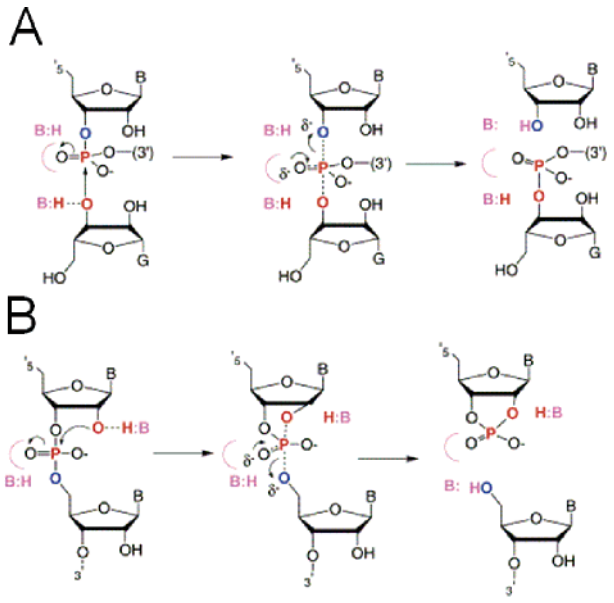

Figure 11. Reactions catalyzed by naturally occurring ribozymes require nucleophilic activation that may be effected by general base chemistry (denoted as B:). Neutralization of negatively charged intermediates (purple arcs) by metal ion interactions is also important. (A) Large ribozymes such as the group I intron catalyze attack of an extrinsic nucleophile at a specific phosphodiester bond. (B) Small ribozymes exemplified by the HDV ribozyme catalyze intramolecular phosphoryl transfer. Reprinted with permission from ref 121. Copyright 2002 Cell Press.

the common, but not necessarily ubiquitous, use of metal ions as a component of nucleophile activation.[122−125] General base catalysis, commonly invoked in protein phosphodiesterases, was first thought to be difficult for RNA, having functional groups with pK_a's far from neutral. However, application of Jencks' libido rule[20] (section 1.4) suggests that this is not a significant limitation, and extensive experimental work has resulted in a greater appreciation of the ability of RNA to employ general base catalysis.

Ribozymes fall into two general classes distinguished by differences in structural complexity and in reaction mechanism (Figure 11). Self-splicing introns, e.g. group I and group II introns, catalyze phosphotransesterification reactions (Figure 11A) using either the 2′-O or 3′-O; and RNase P constitutes a class of large ribozymes. Like their protein counterparts that catalyze similar reactions, such as endonucleases, polymerases, phosphodiesterases, etc., divalent metal ions appear to play a dominant role. The second class, small ribozymes consisting of 70−100 nucleotide structures, catalyzes intramolecular attack of a 2′-OH on the adjacent phosphodiester bond similar to protein ribonucleases such as RNase A (Figure 11B). Small ribozymes are involved in replication of RNA phages as well as several newly discovered classes that are involved in gene regulation. Members of this class can function in the absence of divalent metal ions, and exploration of their mechanisms has shed new light on the capabilities of RNA to effect general base activation of the substrate nucleophile.

2.7. Group I Intron

GI intron splicing involves two successive transesterification reactions. In the first reaction, the active site positions the 3′-O of a free guanosine substrate for nucleophilic attack at the phosphodiester bond of the 5′ splicing site; the 3′-O of the last exon nucleotide is the leaving group. In the second reaction, the 3′-O product from the first reaction attacks the 3′ splice site, generating the spliced exons, and the 3′-O of the last intron nucleotide (gammaG) is the leaving group. An important feature is that the 3′-O leaving group in the first step is the nucleophile for the second step. Similarly, the interactions with the leaving group in the second step will replicate interactions involved in nucleophilic activation in the first step.

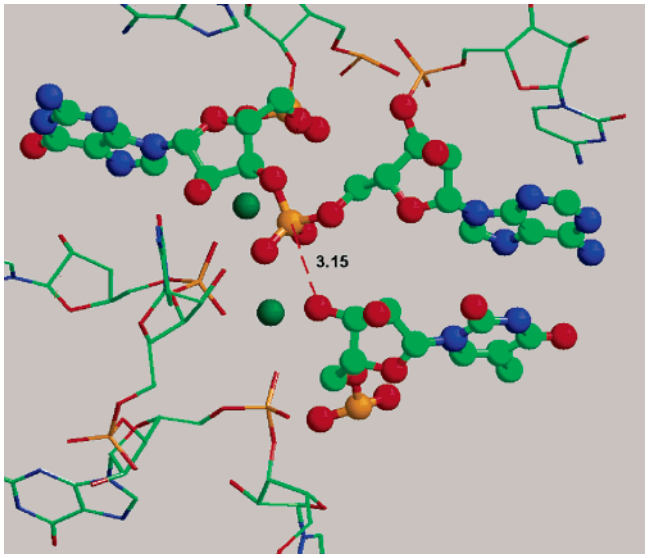

Figure 12. Structure of group I intron adapted from 1ZZN[129] using RasTop.[42] The distance between the nucleophilic 3′-O and the transferred phosphate is depicted. Both the nucleophile and electrophile are within inner sphere distances of the two Mg^{2+} ions (dark green spheres) located at the active site.

Biochemical and structural analysis shows that a conserved helix in the highly structured catalytic core of the GI intron binds the exogenous G nucleophile, as well as the gammaG, for the second step of splicing. The Hoogsteen face of the bound G forms a base triple with a conserved G−C pair where its 3′-O is positioned for nucleophilic attack in the first step. In the second step of splicing, a similar Hoogsteen base pair with gammaG positions the 3′ splice site phosphate for the reverse reaction, i.e., the 3′-O in this step is the leaving group. A recent high-resolution structure of an intermediate, prior to the second step, provides a detailed model of the 3′ splice site substrate interactions that position the appropriate hydroxyl nucleophile and phosphate for the second step.[126−128] Extensive base pairing and tertiary interactions align the exons for the reaction. Notably, the substrate is in a highly constrained conformation with complete reversal of strand direction at the 3′ splice site. The network of hydrogen bonding interactions positions the 3′-OH of the 5′ exon proximal to the scissile phosphate, and the angle of approach is consistent with the geometry expected for inline nucleophilic attack shown in Figure 12.

With respect to active site interactions with the nucleophile/leaving group oxygens, the majority of attention has focused on divalent metal ion interactions, and there is now strong evidence that nucleophilic activation at the 3′-O involves direct coordination to active site Mg^{2+} ions as shown in Figure 12. However, studying metal ion interactions in RNA raises some special problems.[120,124,125] First, structure−function analyses of RNA−metal ion interactions involved in nucleophile activation, or any other aspect of catalysis, are complicated by the necessity of Mg^{2+} ion interactions for folding. Also, RNAs can often fold into more than one energetically favorable ground state conformation and undergo conformational changes. These complications make mechanistic interpretations of structural studies problematic. Importantly, modifications necessary to trap a crystallographic complex prior to catalysis for structural studies may perturb native metal ion interactions. Indeed, in another parallel with protein enzymes, different ribozyme structures can have significant differences in the number and location of metal ions.[130,131] These issues clearly underscore the importance of achieving both high-resolution structural models of these enzymes and extensive correlations with functional studies.

Strong functional evidence for active site metal interactions with the nucleophile comes from pioneering biochemical analyses involving phosphorothioate modifications to test for metal ion interactions.[132−135] In this analysis, functionally deleterious sulfur or nitrogen substitutions that exhibit rescue upon increasing cation softness (e.g., replacing Mg^{2+} with Cd^{2+} or Mn^{2+}) provide evidence for direct metal ion coordination during catalysis.[135,136] The development and most extensive applications of this approach have involved a version of the *Tetrahymena* ribozyme engineered to catalyze the attack of guanosine on a short oligonucleotide substrate. Substrate phosphorothioate-metal ion rescue experiments identified four atoms, including the 3′-O leaving group/nucleophile for both steps. For example, to probe for interaction with the 3′-O nucleophile of the 5′ exon in the second step, a substrate resembling the ligated exons was generated and the enzyme was engineered to catalyze the reverse of the second splicing step. There is a significant rescue for the reaction; thus, by the principle of microscopic reversibility, this metal must interact in the forward reaction with nucleophilic oxygen in the second step.[137]

To gain a more detailed understanding of the relationships between metal ion interactions with the nucleophile and those with other atoms of the reactive phosphate, a thermodynamic fingerprint analysis has been used.[132−135] This extension of the phosphorothioate-rescue approach involves quantitatively analyzing the reactivity of modified substrates relative to unmodified substrates over a range of rescuing metal ion concentrations. The concentration dependence of the relative rates can be interpreted in terms of apparent affinities with magnitudes that serve as distinctive "fingerprints" for the rescuing metal ion(s). Thus, by comparison of these apparent affinities for different modified substrates, information is gained as to whether the same or distinct metal ions interact with the identified substrate ligands. These studies provided functional evidence for a network of three distinct metal ions within the *Tetrahymena* ribozyme active site: Metal ions coordinate to the 3′-oxygen leaving group, the 3′-oxygen on the G nucleophile in the first step (M_A and M_B, respectively), and a third oxygen interacting with the 2′-hydroxyl of the G nucleophile (M_C) (Figure 13). Two metal ions (M_A and M_C) coordinate the *pro*-S_P oxygen of the scissile phosphate, and a third interacts with the nucleophilic 3′O. Extension of this analysis to encompass phosphate oxygens within the intron itself provides evidence that these metal ions are positioned by coordination interactions with nonbridging oxygens that constitute, in part, the active site of the ribozyme.[138,139]

Recently, a structure including the 2′-O of the substrate G, a key metal ion ligand, has been reported, providing the most consistent model to date of active site interactions including metal ion coordination to the 3′-O's involved in nucleophilic attack (Figure 12). In this structure, two metal ions coordinate to nonbridging phosphate oxygens in the intron and substrate. This result seemingly contrasts with the results from biochemical studies that indicate three active site metal ions. However, the two Mg^{2+} ions observed in the three-dimensional structure are able to satisfy all of the biochemically identified interactions, including Mg^{2+} interactions with both 3′-O's. Their geometry is consistent with the

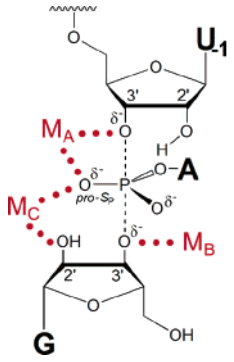

Figure 13. Group I intron splicing reaction. The last nucleotide of the 5′ intron (U-1) is shown at the top. The 3′-O leaving group of this nucleotide serves as the nucleophile for the second splicing step. At the bottom is the exogenous G whose 3′-O serves as the nucleophile. The last nucleotide of the intron (gammaG) occupies this position in the second step of splicing, where its corresponding 3′-O is the leaving group. Metal ion interactions demonstrated by quantitative metal rescue of phosphorothioate modifications are shown in red. Reprinted with permission from ref 138. Copyright Hougland et al.

Steitz two metal ion mechanism from DNA polymerase.[140,141] Importantly, one Mg^{2+} ion makes inner sphere contacts with both the 2′-O and the 3′-O nucleophile/leaving groups of the gammaG. This geometry is consistent with the biochemical data that both positions are ligands for metal ions, but in the crystal structure only a single metal ion is seen coordinating to both ligands. This difference from the mechanism drawn from biochemical data could formally arise from differences in ground state versus transition state interactions or, potentially, differences in the electrostatic environments of the active site due to different functional group modifications. Nonetheless, it is abundantly clear that direct metal coordination to both 3′-O's is a key feature of the catalytic mechanism.

2.8. HDV Ribozyme

In biology, small RNA motifs that catalyze RNA self-cleavage via attack of a ribose 2′-O play essential roles in RNA virus replication, as well as regulation of gene expression. With respect to nucleophilic activation, it has variously been proposed, as with protein enzymes, to involve metal catalysis or general base catalysis via an RNA nucleobase functional group or the water molecule in the inner hydration sphere of Mg^{2+}.[119,120] However, some small ribozymes can function in the absence of divalent metal ions.[142−144] Thus, intensive research has focused on identifying potential general acid/base mechanisms. However, the most detailed models of the catalytic mechanism are built largely on structural rather than functional data. Additionally, there is some conflict between structural studies and the results of detailed functional analyses. Nonetheless, there is significant progress in outlining the distinct geometries for nucleophilic activation in some examples exemplified here by the HDV ribozyme.

The HDV ribozyme is a small ca. 70 nucleotide RNA that, like all small ribozymes, folds to form a compact structure that results in cleavage of a specific phosphodiester bond via attack on the adjacent 2′-O nucleophile.[145] As is the case for protein enzymes such as RNase A that catalyze the same chemistry, the reaction is inhibited by acidic pH, consistent with a deprotonation, potentially of the nucleophile, preceding the rate-limiting step under these conditions.[146,147] Importantly, the HDV ribozyme is able to function in the absence of divalent metal ions, albeit more slowly. Higher monovalent ion concentrations are required for folding, presumably to screen electrostatic repulsion. This result implied that nucleobases could fulfill the role of amino acid side chains in functioning as general acids and bases. Indeed, a growing body of structural and biochemical analyses support that this is in fact the case.

Initial insights into the overall architecture of the ribozymes came from a structure of the 3′ product complex.[148] While this structure did not provide evidence for the interactions with the nucleophile, it showed a nucleobase (C76) potentially positioned for acid−base catalysis. Further physical and mutagenesis studies provided important evidence that the protonation state of C76 is indeed important for catalysis.[149−152] These analyses gave rise to a model in which C76, in its deprotonated form, functions as a general base catalyst to accept a proton from the nucleophilic 2′-O.

Alternatively, C76 could function as a general acid, while a different base catalyst activates the 2′-O nucleophile. Support for this second model came from the observation that the pH dependence of the activity varied with the divalent metal ion concentration, which suggested that the ionization of metal-bound water might contribute to the pH dependence.[147] These results were consistent with the idea that either hydroxide or a metal coordinated hydroxide accepts a proton from the 2′-OH to activate the nucleophile. Additionally, recent experiments investigating the effects of 5′-O leaving group substitutions by Das and Piccirilli further implicate C76 as a general acid catalyst.[153] Recent structures in which C76 has been mutated to U show this residue in position for an interaction with the leaving group, but there is no metal ion in the vicinity of the 2′-O. Such results provide important insights into HDV active site function, but they leave in doubt the precise mechanism of nucleophilic activation in the absence of metal ions. A potential rationale for the slower catalytic activity of the ribozyme under these conditions is that nucleophile deprotonation is not assisted.

It is clear that RNA does not invent new mechanisms for nucleophilic activation or catalysis but is constrained, just as protein enzymes are, to employ those kinds of interactions dictated by the intrinsic chemistry of the reaction. The difference lies in the unique geometries that position RNA functional groups relative to the nucleophile and reactive phosphate in order to stabilize the transition state. These kinds of interactions include employing networks of noncovalent interactions to position the nucleophile in the optimal geometry for in-line attack. RNA is particularly adept at interacting with divalent metal ions, and there is very good evidence for a direct role for active site metal ion coordination in nucleophile activation. Unlike protein enzymes, however, RNA needs metal ions to fold, and the coupling of structure stabilization and catalysis makes achieving a clear picture of the roles of individual interactions challenging. Thus, it is with hindsight that it becomes clear that RNA, despite having a limited repertoire of functional groups, can form an active site environment in which a significant pK_a shift occurs, enabling general acid/base catalysis. Yet, very few examples have been described in any depth, and even for the best characterized examples, there remain important questions concerning the sum total of catalytic interactions and the ultimate effect of active site nucleophile interactions on bonding in the ground state and transition state.

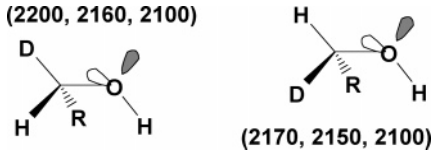

Figure 14. Variation of C−D ν_{str} with H-bonding and ionization. The *anti* (left) and *gauche* (right) C−D bonds of an alcohol have different ν_{str} values. The approximate values given are (in order of decreasing frequency) for the alcohol in $CHCl_3$, i.e., with no H-bond donor or acceptor, complexed to a strong amine base, and as the alkoxide in water.

3. Spectroscopic Characterization of Nucleophiles at Enzyme Active Sites

The previous sections have established that, in the process of binding to enzyme active sites, every alcohol nucleophile has the solvent H-bond donors removed and that the alcohol O−H is either coordinated to an active site general base or, less commonly, deprotonated by coordination to a metal ion. This section focuses on the emerging use of spectroscopic methods to characterize the environment of the nucleophile in enzyme−substrate complexes. In the application of NMR and vibrational spectroscopy, the requisite model studies have now been completed, but the number of applications to the characterization of O nucleophiles in enzyme active sites is very limited.

3.1. Vibrational Spectroscopic Characterization of Alcohols

H-bond strength from alcohols to Bronsted base acceptors has been studied extensively by vibrational spectroscopy. As the H-bond becomes stronger, based on thermodynamic measurements, the O−H stretching frequency (ν_{str}) decreases by several 100 cm^{-1}.[154] While this approach works well in aprotic organic solvents, in aqueous solution, the broad intense band from the solvent O−H stretching modes prevents the identification of the single substrate O−H stretch of interest. This bond cannot be labeled with D, as it exchanges rapidly with solvent and ^{18}O substitution has a minimal effect on the O−H ν_{str}.

To characterize nucleophilicity, the electron density of the lone pairs is more important than the strength of the H-bond. Studies of negative hyperconjugation of C−H bonds vicinal to lone pairs was prompted by the observation that the C−H bond *anti* to a lone pair has a ν_{str} ~30−60 cm^{-1} lower than a C−H bond *anti* to an O−H bond, as shown in Figure 14. H-bond donation by an alcohol increases the electron density around the O, increasing the extent of negative hyperconjugation and decreasing the C−H ν_{str}.[155,156] Ionization of the alcohol to the alkoxide results in a large (>100 cm^{-1}) decrease in the C−H ν_{str}. Unlike the case of the O−H stretch, it is possible to uniquely label a single C−H bond in a substrate by D-substitution. The C−D ν_{str} of 2100−2250 cm^{-1} appears in a spectral window free of both water and protein vibrations. Single C−D bonds can be observed by vibrational spectroscopy in proteins (Maiti, Carey, and Anderson, unpublished), allowing the electron density of a lone pair on a geminal O to be interrogated. The application of vibrational spectroscopy to characterize changes in electron density of substrates bound at active sites has been further reviewed by Carey in this issue.

3.2. NMR Characterization of Alcohol Nucleophiles

NMR has proven to be an extremely valuable tool in characterizing H-bonds between N−H donors and N acceptors. These measurements include characterization of the ^1H chemical shift of the H-bonded proton, its fractionation factor, solvent exchange kinetics, and the scalar coupling constants $^1J_{NH}$ and $^1J_{NN}$. In application to alcohol nucleophiles, many of these NMR observations have not been possible due to the rapid solvent exchange of the H-bonded proton. Even in cases where solvent exchange may be slow, the chemical shift has proven too small to be identifiable from bulk water and the scalar coupling constants, $^1J_{OH}$ to ^{17}O or $^2J_{CH}$, have not been investigated.

However, in favorable cases, O···H···N H-bonded systems can be characterized by the same parameters as N···H···N systems, i.e., the ^1H chemical shift, the fractionation factor, and the $^1J_{NH}$ scalar coupling constant—all of which correlate with the strength of the H-bond.[157] The model experimental systems have focused on aprotic solvents and low temperatures to minimize chemical exchange, and in most systems they have favored zwitterionic complexes with the proton residing closer to the N, i.e., greater N−H than O−H bond order.[158,159] The best characterized O···H···N H-bonded system comes from NMR studies of serine proteases, where the observed ^1H resides between the Asp and the imidazole of the catalytic triad, and is not directly an H-bond donated by the serine nucleophile (reviewed in ref 160). The strongly deshielded proton resonance has a low fractionation factor characteristic of short strong H-bonds.[33] The NMR characterization of this H-bonded system demonstrates the potential for characterizing H-bonds at enzyme active sites, when exchange with solvent has been minimized. Theoretical calculations extend the correlation of chemical shift, fractionation factor, and $^1J_{NH}$ to systems with greater O−H bond order, as anticipated for Ser γO−H···imidazole H-bonds.[161] An alternative approach, based on the observation that the adjacent C−H bond was weakened in H-bond complexes, is to observe the $^1J_{CH}$ of the vicinal methylene protons in alcohol H-bonded systems. A correlation between $^1J_{CH}$ for hexafluoroisopropanol and the H-bond strength formed with amines of varying basicities has been observed.[162]

For O···H···O H-bonded complexes, as observed with carboxylate H-bond acceptors to alcohol nucleophiles in kinases and acyl transferases, the only model NMR study of H-bond parameters comes from fast magic angle spinning determinations of the ^1H chemical shift in crystals where the exchange of the H-bonded protons is minimized and neutron diffraction has characterized the H-bond geometry.[160,163] The chemical shift correlates with the displacement of the ^1H from the middle of the H-bonded system.[164] Except for very strong H-bonds, these methods have not been applied to enzyme systems.

3.3. Isotope Effects on Alcohol Nucleophiles

In characterizing nucleophile activation by isotope effect studies, the most obvious substitution is to label the nucleophilic O with ^{18}O. The effect of removing the H-bond donors can be examined by determining the ^{18}O equilibrium isotope effect on transfer to the gas phase, and this is determined to be small, 1.008.[165] There have been no experimental determinations of the equilibrium isotope effect on alcohols functioning as a donor in forming an H-bonded complex.

As the O−H stretching frequency can be decreased significantly, it is anticipated that forming an H-bond could result in a significant normal equilibrium isotope effect, but computational studies suggest that there is a compensating increase in the C−O bond order.[156] Deprotonation of O−H bonds, however, results in a large normal equilibrium isotope effect; the ^{18}O effect on ionization of water is 1.04.[166] Metal ion coordination, by introducing a new bond to the alcohol O, results in an inverse ^{18}O equilibrium isotope effect of 0.98 for coordination to a divalent metal ion.[167] The presence of an inverse ^{18}O isotope effect on binding of an alcohol to an enzyme active site would be strongly suggestive of coordination to a metal ion. These small ^{18}O isotope effects on binding can be measured with sufficient precision by whole molecule mass spectrometry.[168−170] Thus, both ionization and metal ion coordination of an oxygen nucleophile should give rise to a readily interpretable ^{18}O isotope effect on binding.

Since equilibrium isotope effects are generated by changes in vibrational frequencies between the substrate and product states, the measurement of these effects can be considered a subsidiary of vibrational spectroscopy. The advantages of determining the isotope effects are that they can be measured with a trace label and with minimal material employed at low concentrations and that *kinetic* isotope effects provide insight into the transition state of a reaction, a capability effectively unavailable to any other spectroscopic method. The disadvantage of isotope effect determinations is that all of the vibrational modes of the isotopically substituted atom can contribute to the measured effect,[171] not just the stretching vibration of major interest.

The decrease in the ν_{str} of a C−D bond of a substrate on formation of the Michaelis complex, as predicted to occur on formation of a strong H-bond, will contribute to a normal equilibrium isotope effect on association of the substrate. These equilibrium binding isotope effects have been predicted[87,156] and observed.[84−86,172] For hexokinase, there is a significant isotope effect of 1.06 measured with [6−^{3}H]-glucose.[85] This normal effect is interpreted as suggesting that the active site Asp657 forms a significant H-bond to promote the nucleophilicity of the C6 hydroxyl group even in the binary enzyme−glucose complex. The value is inconsistent with ionization of the C6 hydroxyl, as ionization of alcohols results in significantly larger equilibrium isotope effects, >1.15.[88,156,173]

Unexpectedly large 5′-3H kinetic isotope effects have been observed in enzymes catalyzing the cleavage of the glycosidic bond in nucleosides.[174,175] These results, while attributed to interactions present in the Michaelis complex,[176] are indicative of the ability to observe changes in the electronic distribution about an alcohol in the transition state. Preequilibrium ionization will result in large secondary kinetic isotope effects and should provide a diagnostic for this mechanism. In the serine transacetylase reaction, [3−^{2}H]-serine kinetic isotope effects have been determined to be near unity, indicating that in this reaction the serine has not been deprotonated in the rate-determining transition state.[74]

4. Acknowledgments

This review was supported in part by NIH Grant GM56740, NSF Grant MCB-0110610, and the Medical Scientist Training Program at Case Western Reserve University.

5. References

(1) Swain, C. G.; Scott, C. B. *J. Am. Chem. Soc.* **1953**, *75*, 141.
(2) Pearson, R. G.; Sobel, H. R.; Songstad, J. *J. Am. Chem. Soc.* **1968**, *90*, 319.
(3) Zhang, X.; Houk, K. N. *Acc. Chem. Res.* **2005**, *38*, 379.
(4) Jencks, W. P.; Gilchrist, M. *J. Am. Chem. Soc.* **1968**, *90*, 2622.
(5) Honig, B.; Nicholls, A. *Science* **1995**, *268*, 1144.
(6) Belasco, J. G.; Knowles, J. R. *Biochemistry* **1980**, *19*, 472.
(7) D'Ordine, R. L.; Pawlak, J.; Bahnson, B. J.; Anderson, V. E. *Biochemistry* **2002**, *41*, 2630.
(8) Deng, H.; Lewandowicz, A.; Schramm, V. L.; Callender, R. *J. Am. Chem. Soc.* **2004**, *126*, 9516.
(9) Alexander, R.; Ko, E. C. F.; Parker, A. J.; Broxton, T. J. *J. Am. Chem. Soc.* **1968**, *90*, 5049.
(10) Adamovic, I.; Gordon, M. S. *J. Phys. Chem. A* **2005**, *109*, 1629.
(11) Acevedo, O.; Jorgensen, W. L. *Org. Lett.* **2004**, *6*, 2881.
(12) Freccero, M.; Di Valentin, C.; Sarzi-Amade, M. *J. Am. Chem. Soc.* **2003**, *125*, 3544.
(13) Re, S.; Morokuma, K. *J. Phys. Chem. A* **2001**, *105*, 7185.
(14) Jencks, W. P. *Adv. Chem. Ser.* **1987**, *215* (Nucleophilicity), 155.
(15) Jencks, W. P.; Haber, M. T.; Herschlag, D.; Nazaretian, K. L. *J. Am. Chem. Soc.* **1986**, *108*, 479.
(16) Rucker, V. C.; Byers, L. D. *J. Am. Chem. Soc.* **2000**, *122*, 8365.
(17) Onyido, I.; Swierczek, K.; Purcell, J.; Hengge, A. C. *J. Am. Chem. Soc.* **2005**, *127*, 7703.
(18) Olsson, M. H. M.; Warshel, A. *J. Am. Chem. Soc.* **2004**, *126*, 15167.
(19) Warshel, A.; Aqvist, J.; Creighton, S. *Proc. Natl. Acad. Sci., U.S.A.* **1989**, *86*, 5820.
(20) Jencks, W. P. *J. Am. Chem. Soc.* **1972**, *94*, 4731.
(21) Swain, C. G.; Kuhn, D. A.; Schowen, R. L. *J. Am. Chem. Soc.* **1965**, *87*, 1553.
(22) Knipe, J.; Coward, J. K. *J. Am. Chem. Soc.* **1979**, *101*, 4339.
(23) Dietze, P. E.; Jencks, W. P. *J. Am. Chem. Soc.* **1989**, *111*, 340.
(24) Strajbl, M.; Florian, J.; Warshel, A. *J. Am. Chem. Soc.* **2000**, *122*, 5354.
(25) Hibbert, F.; Emsley, J. *Advances in Physical Organic Chemistry*; Bethell, D., Ed.; Academic Press: New York, 1990; Vol. 26.
(26) Del Bene, J. E.; Jordan, M. J. T. *Int. Rev. Phys. Chem.* **1999**, *18*, 119.
(27) Kuhn, P.; Knapp, M.; Soltis, S. M.; Ganshaw, G.; Thoene, M.; Bott, R. *Biochemistry* **1998**, *37*, 13446.
(28) Rypniewski, W. R.; Ostergaard, P. R.; Norregaard-Madsen, M.; Dauter, M.; Wilson, K. S. *Acta Crystallogr., Sect. D: Biol. Crystallogr.* **2001**, *57*, 8.
(29) Quinn, D. M.; Sutton, L. D. In *Enzyme Mechanism from Isotope Effects*; Cook, P. F., Ed.; CRC Press: Boca Raton, FL, 1991.
(30) Cordes, E. H. *Prog. Phys. Org. Chem.* **1967**, *4*, 1.
(31) Eliason, R.; Kreevoy, M. M. *J. Am. Chem. Soc.* **1978**, *100*, 7037.
(32) Schowen, K. B.; Limbach, H. H.; Denisov, G. S.; Schowen, R. L. *Biochim. Biophys. Acta* **2000**, *1458*, 43.
(33) Lin, J.; Westler, W. M.; Cleland, W. W.; Markley, J. L.; Frey, P. A. *Proc. Natl. Acad. Sci., U.S.A.* **1998**, *95*, 14664.
(34) Dougherty, T. M.; Cleland, W. W. *Biochemistry* **1985**, *24*, 5875.
(35) Larsen, T. M.; Benning, M. M.; Rayment, I.; Reed, G. H. *Biochemistry* **1998**, *37*, 6247.
(36) Lerner, C.; Masjost, B.; Ruf, A.; Gramlich, V.; Jakob-Roetne, R.; Zurcher, G.; Borroni, E.; Diederich, F. *Org. Biomol. Chem.* **2003**, *1*, 42.
(37) Adams, J. A. *Chem. Rev.* **2001**, *101*, 2271.
(38) Kemp, B. E.; Benjamini, E.; Krebs, E. G. *Proc. Natl. Acad. Sci., U.S.A.* **1976**, *73*, 1038.
(39) Kemp, B. E.; Graves, D. J.; Benjamini, E.; Krebs, E. G. *J. Biol. Chem.* **1977**, *252*, 4888.
(40) Hanks, S. K.; Quinn, A. M.; Hunter, T. *Science* **1988**, *241*, 42.
(41) Madhusudan; Trafny, E. A.; Xuong, N. H.; Adams, J. A.; Ten Eyck, L. F.; Taylor, S. S.; Sowadski, J. M. *Protein Sci.* **1994**, *3*, 176.
(42) Zheng, J.; Knighton, D. R.; Ten Eyck, L. F.; Karlsson, R.; Xuong, N.; Taylor, S. S.; Sowadski, J. M. *Biochemistry* **1993**, *32*, 2154.
(43) Biology, N. S.; Madhusudan; Akamine, P.; Xuong, N. H.; Taylor, S. S. *Nat. Struct. Biol.* **2002**, *9*, 273.
(44) Valadon, P.; Bernstein, H. J. *RasTop*, Version 1.3.1; 2001.
(45) Gibbs, C. S.; Zoller, M. J. *J. Biol. Chem.* **1991**, *266*, 8923.
(46) Skamnaki, V. T.; Owen, D. J.; Noble, M. E. M.; Lowe, E. D.; Lowe, G.; Oikonomakos, N. G.; Johnson, L. N. *Biochemistry* **1999**, *38*, 14718.
(47) Zhou, J.; Adams, J. A. *Biochemistry* **1997**, *36*, 2977.
(48) Yoon, M. Y.; Cook, P. F. *Biochemistry* **1987**, *26*, 4118.
(49) Ho, M.; Bramson, H. N.; Hansen, D. E.; Knowles, J. R.; Kaiser, E. T. *J. Am. Chem. Soc.* **1988**, *110*, 2680.
(50) Knighton, D. R.; Zheng, J.; Ten Eyck, L. F.; Ashford, V. A.; Xuong, N.; Taylor, S. S.; Sowadski, J. M. *Science* **1991**, *253*, 407.
(51) Adams, J. A.; Taylor, S. S. *J. Biol. Chem.* **1993**, *268*, 7747.

(52) Adams, J. A.; Taylor, S. S. *Biochemistry* **1992**, *31*, 8516.
(53) Grant, B. D.; Adams, J. A. *Biochemistry* **1996**, *35*, 2022.
(54) Jencks, W. F. *Catalysis in Chemistry and Enzymology*; McGraw-Hill: New York, 1969.
(55) Hirano, Y.; Masayuki, H.; Hoshino, T.; Tsuda, M. *J. Phys. Chem. B* **2002**, *106*, 5788.
(56) Hart, J. C.; Sheppard, D. W.; Hillier, I. H.; Burton, N. A. *Chem. Commun.* **1999**, *1999*, 79.
(57) Hutter, M. C.; Helms, V. *Protein Sci.* **1999**, *8*, 2728.
(58) Valiev, M.; Kawai, R.; Adams, J. A.; Weare, J. H. *J. Am. Chem. Soc.* **2003**, *125*, 9926.
(59) Diaz, N.; Field, M. J. *J. Am. Chem. Soc.* **2004**, *126*, 529.
(60) Cheng, Y.; Zhang, Y.; McCammon, J. A. *J. Am. Chem. Soc.* **2005**, *127*, 1553.
(61) Johnson, C. M.; Roderick, S. L.; Cook, P. F. *Arch. Biochem. Biophys.* **2005**, *433*, 85.
(62) Kredich, N. M.; Tomkins, G. M. *J. Biol. Chem.* **1966**, *241*, 4955.
(63) Kredich, N. M.; Becker, M. A.; Tomkins, G. M. *J. Biol. Chem.* **1969**, *244*, 2428.
(64) Olsen, L. R.; Huang, B.; Vetting, M. W.; Roderick, S. L. *Biochemistry* **2004**, *43*, 6013.
(65) Pye, V. E.; Tingey, A. P.; Robson, R. L.; Moody, P. C. E. *J. Biol. Chem.* **2004**, *279*, 40729.
(66) Blow, D. M.; Birktoft, J. J.; Hartley, B. S. *Nature* **1969**, *221*, 337.
(67) Hedstrom, L. *Chem. Rev.* **2002**, *102*, 4501.
(68) Hindson, V. J.; Shaw, W. V. *Biochemistry* **2003**, *42*, 3113.
(69) Hindson, V. J. *Biochem. J.* **2003**, *375*, 745.
(70) Johnson, C. M.; Huang, B.; Roderick, S. L.; Cook, P. F. *Biochemistry* **2004**, *43*, 15534.
(71) Wyckoff, T. J. O.; Raetz, C. R. H. *J. Biol. Chem.* **1999**, *274*, 27047.
(72) Lewendon, A.; Murray, I. A.; Shaw, W. V. *Biochemistry* **1994**, *33*, 1944.
(73) Murray, I. A.; Shaw, W. V. *Antimicrob. Agents Chemother.* **1997**, *41*, 1.
(74) Ruszczycky, M. W. Ph.D. Thesis, Case Western Reserve University, 2006.
(75) Ruszczycky, M. W.; Anderson, V. E. Unpublished work.
(76) Anderson, C. M.; Stenkamp, R. E.; McDonald, R. C.; Steitz, T. A. *J. Mol. Biol.* **1978**, *123*, 207.
(77) Viola, R. E.; Cleland, W. W. *Biochemistry* **1978**, *17*, 4111.
(78) Bohnensack, R.; Hofmann, E. *Eur. J. Biochem.* **1969**, *9*, 534.
(79) Arora, K. K.; Filburn, C. R.; Pedersen, P. L. *J. Biol. Chem.* **1991**, *266*, 5359.
(80) Lange, A. J.; Xu, L. Z.; van Poelwijk, F.; Lin, K.; Granner, D. K.; Pilkis, S. J. *Biochem. J.* **1991**, *277*, 159.
(81) Wilkinson, K. D.; Rose, I. A. *J. Biol. Chem.* **1979**, *254*, 12567.
(82) Taylor, K. B.; Cook, P. F.; Cleland, W. W. *Eur. J. Biochem.* **1983**, *134*, 571.
(83) Cornish-Bowden, A.; Pollard-Knight, D. *Arch. Biol. Med. Exp. (Santiago)* **1985**, *18*, 293.
(84) Lewis, B. E.; Schramm, V. L. In *Isotope Effects in Chemistry and Biology*; Kohen, A., Limbach, H.-H., Eds.; CRC Press: Boca Raton, FL, 2006.
(85) Lewis, B. E.; Schramm, V. L. *J. Am. Chem. Soc.* **2003**, *125*, 4785.
(86) Lewis, B. E.; Schramm, V. L. *J. Am. Chem. Soc.* **2003**, *125*, 4672.
(87) Lewis, B. E.; Schramm, V. L. *J. Am. Chem. Soc.* **2001**, *123*, 1327.
(88) Lewis, B. E.; Schramm, V. L. *J. Am. Chem. Soc.* **2003**, *125*, 7872.
(89) Bender, M. L. *J. Am. Chem. Soc.* **1962**, *84*, 2582.
(90) Voet, D.; Voet, J. G. *Biochemistry*, 2nd ed.; John Wiley & Sons: New York, 1995.
(91) Bender, M. L.; Clement, C. E.; Kezdy, F. J.; Heck, H. D. A. *J. Am. Chem. Soc.* **1964**, *86*, 3680.
(92) Kezdy, F. J.; Bender, M. L. *Biochemistry* **1962**, *1*, 1097.
(93) Gutfreund, H.; Sturtevant, J. M. *Proc. Natl. Acad. Sci., U.S.A.* **1956**, *42*, 719.
(94) Frigerio, F.; Coda, A.; Pugliese, L.; Lionetti, C.; Menegatti, E.; Amiconi, G.; Schnebli, H. P.; Ascenzi, P.; Bolognesi, M. *J. Mol. Biol.* **1992**, *225*, 107.
(95) Bender, M. L.; Hamilton, G. A. *J. Am. Chem. Soc.* **1962**, *84*, 2570.
(96) Bender, M. L.; Pollock, E. J.; Neveu, M. C. *J. Am. Chem. Soc.* **1962**, *84*, 595.
(97) Elrod, J. P.; Hogg, J. L.; Quinn, D. M.; Venkatasubban, K. S.; Schowen, R. L. *J. Am. Chem. Soc.* **1980**, *102*, 3917.
(98) Zerner, B.; Bond, R. P. M.; Bender, M. L. *J. Am. Chem. Soc.* **1964**, *86*, 3674.
(99) Hunkapiller, M. W.; Forgac, M. D.; Richards, J. H. *Biochemistry* **1976**, *15*, 5581.
(100) Quinn, D. M.; Elrod, J. P.; Ardis, R.; Friesen, P.; Schowen, R. L. *J. Am. Chem. Soc.* **1980**, *102*, 5358.
(101) Stein, R. L. *J. Am. Chem. Soc.* **1983**, *105*, 5111.
(102) Enyedy, E. J.; Kovach, I. M. *J. Am. Chem. Soc.* **2004**, *126*, 6017.
(103) Zhang, D.; Kovach, I. M. *J. Am. Chem. Soc.* **2005**, *127*, 3760.
(104) Ishida, T.; Kato, S. *J. Am. Chem. Soc.* **2003**, *125*, 12035.
(105) Ishida, T.; Kato, S. *J. Am. Chem. Soc.* **2004**, *126*, 7111.
(106) Lu, Y.; Handoo, K. L.; Parker, V. D. *Org. Biomol. Chem.* **2003**, *1*, 36.
(107) Kevill, D. N.; Kim, C. B. *Bull. Soc. Chim. Fr.* **1988**, 383.
(108) Breslow, R.; Groves, K.; Mayer, M. U. *J. Am. Chem. Soc.* **2002**, *124*, 3622.
(109) Lerner, C.; Ruf, A.; Gramlich, V.; Masjost, B.; Zurcher, G.; Jakob-Roetne, R.; Borroni, E.; Diederich, F. *Angew. Chem., Int. Ed. Engl.* **2001**, *40*, 4040.
(110) Ruggiero, G. D.; Williams, I. H.; Roca, M.; Moliner, V.; Tunon, I. *J. Am. Chem. Soc.* **2004**, *126*, 8634.
(111) Rodgers, J.; Femec, D. A.; Schowen, R. L. *J. Am. Chem. Soc.* **1982**, *104*, 3263.
(112) Lau, E. Y.; Bruice, T. C. *J. Am. Chem. Soc.* **1998**, *120*, 12387.
(113) Knipe, J. O.; Vasquez, P. J.; Coward, J. K. *J. Am. Chem. Soc.* **1982**, *104*, 3202.
(114) Kuhn, B.; Kollman, P. A. *J. Am. Chem. Soc.* **2000**, *122*, 2586.
(115) Lau, E. Y.; Bruice, T. C. *J. Am. Chem. Soc.* **2000**, *122*, 7165.
(116) Roca, M.; Marti, S.; Andres, J.; Moliner, V.; Tunon, I.; Bertran, J.; Williams, I. H. *J. Am. Chem. Soc.* **2003**, *125*, 7726.
(117) Seibert, C. M.; Raushel, F. M. *Biochemistry* **2005**, *44*, 6383.
(118) Herschlag, D. *Nature* **1998**, *395*, 548.
(119) Doudna, J. A.; Lorsch, J. R. *Nat. Struct. Mol. Biol.* **2005**, *12*, 395.
(120) Fedor, M. J.; Williamson, J. R. *Nat. Rev. Mol. Cell Biol.* **2005**, *6*, 399.
(121) DeRose, V. J. *Chem. Biol.* **2002**, *9*, 961.
(122) Doudna, J. A.; Cech, T. R. *Nature* **2002**, *418*, 222.
(123) Hanna, R.; Doudna, J. A. *Curr. Opin. Chem. Biol.* **2000**, *4*, 166.
(124) Pyle, A. M. *J. Biol. Inorg. Chem.* **2002**, *7*, 679.
(125) DeRose, V. J. *Curr. Opin. Struct. Biol.* **2003**, *13*, 317.
(126) Stahley, M. R.; Strobel, S. A. *Science* **2005**, *309*, 1587.
(127) Adams, P. L.; Stahley, M. R.; Gill, M. L.; Kosek, A. B.; Wang, J.; Strobel, S. A. *RNA* **2004**, *10*, 1867.
(128) Adams, P. L.; Stahley, M. R.; Kosek, A. B.; Wang, J.; Strobel, S. A. *Nature* **2004**, *430*, 45.
(129) Stahley, M. R.; Strobel, S. A. *Science* **2005**, *309*, 1587.
(130) Vicens, Q.; Cech, T. R. *Trends Biochem. Sci.* **2005**, *12*, 12.
(131) Guo, F.; Gooding, A. R.; Cech, T. R. *Mol. Cell* **2004**, *16*, 351.
(132) Shan, S.; Kravchuk, A. V.; Piccirilli, J. A.; Herschlag, D. *Biochemistry* **2001**, *40*, 5161.
(133) Yoshida, A.; Sun, S.; Piccirilli, J. A. *Nat. Struct. Biol.* **1999**, *6*, 318.
(134) Shan, S.; Yoshida, A.; Sun, S.; Piccirilli, J. A.; Herschlag, D. *Proc. Natl. Acad. Sci., U.S.A.* **1999**, *96*, 12299.
(135) Piccirilli, J. A.; Vyle, J. S.; Caruthers, M. H.; Cech, T. R. *Nature* **1993**, *361*, 85.
(136) Jaffe, E. K.; Markham, G. D. *Biochemistry* **1987**, *26*, 4258.
(137) Weinstein, L. B.; Jones, B. C.; Cosstick, R.; Cech, T. R. *Nature* **1997**, *388*, 805.
(138) Hougland, J. L.; Kravchuk, A. V.; Herschlag, D.; Piccirilli, J. A. *PLoS Biol.* **2005**, *3*, e277. Epub 2005 Aug 16.
(139) Szewczak, A. A.; Kosek, A. B.; Piccirilli, J. A.; Strobel, S. A. *Biochemistry* **2002**, *41*, 2516.
(140) Beese, L. S.; Steitz, T. A. *EMBO J.* **1991**, *10*, 25.
(141) Steitz, T. A.; Steitz, J. A. *Proc. Natl. Acad. Sci., U.S.A.* **1993**, *90*, 6498.
(142) Murray, J. B.; Seyhan, A. A.; Walter, N. G.; Burke, J. M.; Scott, W. G. *Chem. Biol.* **1998**, *5*, 587.
(143) Curtis, E. A.; Bartel, D. P. *RNA* **2001**, *7*, 546.
(144) Nakano, S.; Proctor, D. J.; Bevilacqua, P. C. *Biochemistry* **2001**, *40*, 12022.
(145) Shih, I. H.; Been, M. D. *Annu. Rev. Biochem.* **2002**, *71*, 887.
(146) Bevilacqua, P. C.; Brown, T. S.; Nakano, S.; Yajima, R. *Biopolymers* **2004**, *73*, 90.
(147) Nakano, S.; Chadalavada, D. M.; Bevilacqua, P. C. *Science* **2000**, *287*, 1493.
(148) Ferre-D'Amare, A. R.; Zhou, K.; Doudna, J. A. *Nature* **1998**, *395*, 567.
(149) Kumar, P. K.; Suh, Y. A.; Miyashiro, H.; Nishikawa, F.; Kawakami, J.; Taira, K.; Nishikawa, S. *Nucleic Acids Res.* **1992**, *20*, 3919.
(150) Perrotta, A. T.; Shih, I.; Been, M. D. *Science* **1999**, *286*, 123.
(151) Shih, I. H.; Been, M. D. *Proc. Natl. Acad. Sci., U.S.A.* **2001**, *98*, 1489.
(152) Suh, Y. A.; Kumar, P. K.; Kawakami, J.; Nishikawa, F.; Taira, K.; Nishikawa, S. *FEBS Lett.* **1993**, *326*, 158.
(153) Das, S. R.; Fong, R.; Piccirilli, J. A. *Curr. Opin. Chem. Biol.* **2005**, *9*, 585.
(154) Piaggio, P.; Tubino, R.; Dellepiane, C. *J. Mol. Struct.* **1983**, *96*, 277.
(155) Maiti, N. C.; Carey, P. R.; Anderson, V. E. *J. Phys. Chem. A* **2003**, *107*, 9910.
(156) Gawlita, E.; Lantz, M.; Paneth, P.; Bell, A.; Tonge, P.; Anderson, V. E. *J. Am. Chem. Soc.* **2000**, *122*, 11660.

(157) Limbach, H. H.; Pietrzak, M.; Sharif, S.; Tolstoy, P. M.; Shenderovich, I. G.; Smirnov, S. N.; Golubev, N. S.; Denisov, G. S. *Chemistry* **2004**, *10*, 5195.
(158) Tolstoy, P. M.; Smirnov, S. N.; Shenderovich, I. G.; Golubev, N. S.; Denisov, G. S.; Limbach, H.-H. *J. Mol. Struct.* **2004**, *700*, 19.
(159) Janke, E. M. B.; Limbach, H.-H.; Weisz, K. *J. Am. Chem. Soc.* **2004**, *126*, 2135.
(160) Harris, T. K.; Mildvan, A. S. *Proteins* **1999**, *35*, 275.
(161) Limbach, H.-H.; Pietrzak, M.; Sharif, S.; Tolstoy, P. M.; Shenderovich, I. G.; Smirnov, S. N.; Golubev, N. S.; Denisov, G. S. *Chem.*−*Eur. J.* **2004**, *10*, 5195.
(162) Maiti, N. C.; Zhu, Y.; Carmichael, I.; Serianni, A. S.; Anderson, V. E. *J. Org. Chem.* **2006**, *71*, 2878.
(163) McDermott, A.; Ridenour, C. F. *Encyclopedia of NMR*; Wiley: Sussex, U.K., 1996; pp 3820−3825.
(164) Emmler, T.; Gieschler, S.; Limbach, H. H.; Buntkowsky, G. *J. Mol. Struct.* **2004**, *700*, 29.
(165) Jansco, G.; Van Hook, W. A. *Chem. Rev.* **1974**, *74*, 689.
(166) Green, M.; Taube, H. *J. Phys. Chem.* **1963**, *67*, 1565.
(167) Feder, H. M.; Taube, H. *J. Chem. Phys.* **1952**, *20*, 1335.
(168) Gawlita, E.; Anderson, V. E.; Paneth, P. *Biochemistry* **1995**, *34*, 6050.
(169) Cassano, A. G.; Anderson, V. E.; Harris, M. E. *J. Am. Chem. Soc.* **2002**, *124*, 10964.
(170) Cassano, A. G.; Anderson, V. E.; Harris, M. E. *Biochemistry* **2004**, *43*, 10547.
(171) Bigeleisen, J.; Wolfsberg, M. *Adv. Chem. Phys.* **1958**, *1*, 15.
(172) LaReau, R. D.; Wan, W.; Anderson, V. E. *Biochemistry* **1989**, *28*, 3619.
(173) DeFrees, D. J.; Taagepera, M.; Levi, B. A.; Pollack, S. K.; Summerhays, K. D.; Taft, R. W.; Wolfsberg, M.; Hehre, W. J. *J. Am. Chem. Soc.* **1979**, *101*, 5532.
(174) Birck, M. R.; Schramm, V. L. *J. Am. Chem. Soc.* **2004**, *126*, 2447.
(175) Horenstein, B. A.; Parkin, D. W.; Estupinan, B.; Schramm, V. L. *Biochemistry* **1991**, *30*, 10788.
(176) Birck, M. R.; Schramm, V. L. *J. Am. Chem. Soc.* **2004**, *126*, 6882.

CR050281Z